Exergy Analysis of Biomass Gasification by Using Computational Method

By

Ahsan Ayub
Reg # 00000205044
Session 2017-2019

Supervised by
Dr. Muhammad Hassan

A Thesis Submitted to the US Pakistan Centre for Advanced Studies in Energy in partial fulfillment of the requirements of the degree of

MASTER of SCIENCE in
THERMAL ENERGY ENGINEERING

US-Pakistan Centre for Advanced Studies in Energy (USPCAS-E)
National University of Sciences and Technology (NUST)

H-12, Islamabad 44000, Pakistan

April 2021

THESIS ACCEPTANCE CERTIFICATE

Certified that final copy of MS thesis written by Ahsan Ayub (Registration No. 00000205044), of U.S.-Pakistan Centre for Advanced Studies in Energy has been vetted by undersigned, found complete in all respects as per NUST Statues/Regulations, is within the similarity indices limit and accepted as partial fulfillment for the award of MS/MPhil degree. It is further certified that necessary amendments as pointed out by GEC members of the scholar have also been incorporated in the said thesis.

Signature: _____

Name of Supervisor: Dr. Muhammad Hassan

Date: _____

Signature (HOD): _____

Date: _____

Signature (Dean/Principal): _____

Date: _____

Certificate

This is to certify that work in this thesis has been carried out by **Mr. Ahsan Ayub** and completed under my supervision in, US-Pakistan Center for Advanced Studies in Energy (USPCAS-E), National University of Sciences and Technology, H-12, Islamabad, Pakistan.

Supervisor: _____

Dr. Muhammad Hassan
USPCAS-E
NUST, Islamabad

Co-supervisor (GEC member # 1): _____

Dr. Iftikhar Ahmad
SCME
NUST, Islamabad

GEC member # 2: _____

Dr. Majid Ali
USPCAS-E
NUST, Islamabad

GEC member # 3: _____

Dr. Muhammad Ahsan
SCME
NUST, Islamabad

HOD-Thermal Energy Engineering: _____

Dr. Adeel Javed
USPCAS-E
NUST, Islamabad

Principal/ Dean: _____

Dr. Adeel Waqas
USPCAS-E
NUST, Islamabad

Acknowledgments

All praise to Allah Almighty who gave me the strength and knowledge to do the work presented in this thesis.

This dissertation would not have been possible without the guidance and the help of several individuals who in one way or another contributed, and extended their valuable assistance in the preparation and completion of this study.

I want to acknowledge Dr. Muhammad Hassan and Dr. Iftikhar Ahmad's profound supervision and guidance throughout this research and thesis. Their professional approach towards a problem can only be surpassed by his friendly supervision that has brought the best out of me. He polished my research skills and I have learned a lot under his supervision and guidance.

I would also like to thanks my GEC committee members, Dr. Majid Ali and Dr. Muhammad Ahsan who honored my committee’s presence.

Finally, my appreciation also goes to my family and friends for their encouragement, love, and support throughout my life.

Abstract

Biomass gasification is an emerging technology for the production of synthesis gas. A robust mechanism for evaluating its energy efficiency is vital to realize the biomass gasification process's efficient operation. In this context, exergy based analysis has been getting more attention from researchers over conventional energy-based analysis because of its capability to encompasses the effect of all the irreversibilities present in a process. In this study, the exergy analysis of the biomass gasifier was performed in computational fluid dynamics (CFD) environment. For the model development, the designed specifications of a lab-scale downdraft biomass gasifier were used. The reaction sets were imported from the species transport model. A code for exergy analysis was written in a custom field function (CFF). The designed model achieved better syngas composition and gasification temperature compared to reported work in literature. The algorithm for exergy analysis also helped in evaluating the downdraft biomass gasifier's performance by analyzing all three types of exergies, chemical exergy, physical exergy, and mixing exergy.

Keywords: downdraft biomass gasifier, computational fluid dynamics, chemical exergy, mixing exergy, physical exergy, custom field function

Table of Contents

List of Figures

List of Tables

Abbreviations

CFD	Computational Fluid Dynamics
CFF	Custom Field Function
GHG	Greenhouse Gas
CCS	Carbon Capture Storage
E^{PH}	Physical Exergy
E^{CH}	Chemical Exergy
E^{mix}	Mixing Exergy

Chapter 1: Introduction

Fossil fuels are considered a significant source of energy. Worldwide, 80% of energy is obtained from fossil fuels [1]. The growing demand for energy production from fossil fuels leads to global warming, air pollution and health concerns. The ever increasing environmental impact divert the researcher's interest in exploring alternative sources[1], [2]. Primary alternative energy sources are, bioenergy, wind, solar, nuclear and hydropower, etc [3]. Bioenergy is produced from renewable sources, such as wood waste, animal waste, grain dust, crop residues, fruit tree, vegetable oils, wheat, sugar beet, corn, straw, and municipal solid waste [4]. The conversion from feedstock to bioenergy can be carried out by biomass gasification, mixed culture biotechnology, anaerobic fermentation process, micro-algal biorefinery, anaerobic digestion microbiome, and transesterification of vegetable oil [5]–[9]. Among sustainable energy sources, biomass is considered as an alternative energy source due to its reduced carbon emissions [10]. The reduction of greenhouse gas (GHG) emissions is only possible by retrieving a carbon-neutral fuel, as shown in Figure 1[11].

Since the 18^{th} Century, energy generation through biomass gasification has been used. Mostly, wooden based biomass has gained more attention from researchers. The wooden feedstock of biomass has low calorific values, but its sustainable nature attracts researchers [12]. Biomass gasification is the thermal conversion of feedstock to synthesis gas [13]. The biomass gasification process focuses on research to get high fuel quality, energy-efficient and economically viable operation. Computational methods have played a major role in realizing efficient process design. Several studies based on the computational method of biomass gasification have been reported to literature in this context. These studies have been performed in different computational methods such as MATLAB [14]–[16], Aspen [16]–[18], CFD [19]–[24]. The CFD advantage over other tools is that it can simulate the physical process at any specific conditions and examine any particular region of interest.

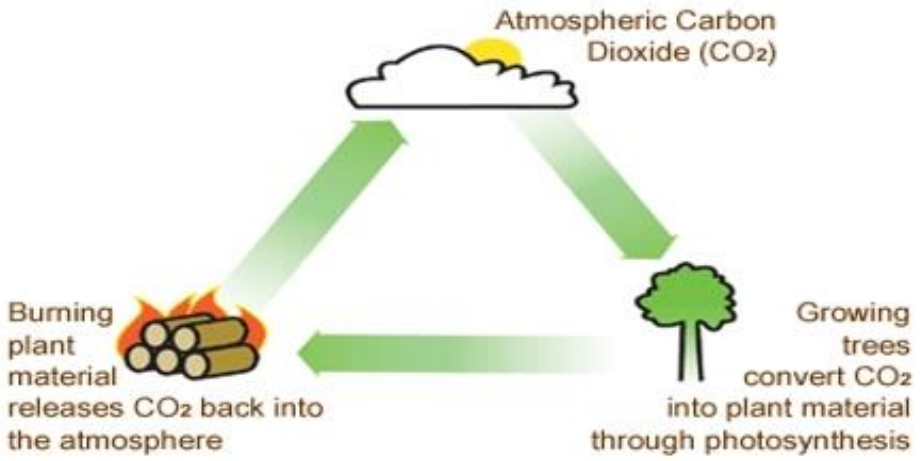

Figure 1: Carbon Neutral Fuel

1.1 Literature Review

Kong et.al, 2008, developed a MATLAB® program to provide the solution for the boundary values problem of biomass gasification and the model is also validated with experimental results. The model's limitations are one dimensional, small biomass particles, and long and thin fluidized bed reactors. Due to these limitations the model can't be used for extensive model validations [15]. Damiani et.al, 2010, performed a data-based prediction of the experimental biomass gasification model to better predict output variables by using MATLAB-Simulink® [14]. Collazo et.al, 2012, analyzed the biomass boiler's main parameters by using the CFD model. This model can also be implemented on different reactors in which reaction time is more significant. The model was developed under highly stirred reactor conditions and constant temperature at devolatilization and char combustion [19]. Gomez et.al, 2014, simulated the transient combustion of three dimensional packed bed gasifier by using Ansys Fluent. An experimental model is also validated by simulating it in Ansys fluent by variant air mass flow rate to examine the evolution of main variables on combustion i.e. ignition rates, char components, devolatilization, etc. [20]. Gomez, et.al, 2015, simulated the up-to-date biomass boiler by variant conditions to obtain a steady-state process. Eulerian and species transport model is used for solid particles and thermal conversion of solid particles [21]. Barsali, et.al, 2015, developed a simulator of combustion process in which evolution of gas flow and the solid consumption is studied during the chemical reaction. This studies conclude

that the physical modelling approach combines with the simulator to provide best behavior of the system [25]. Ismail, et.al, 2015, developed model for updraft biomass gasifier as shown in Figure 1.2, in order to analyze the temperature pressure profile, species concentration. However, the sensitivity analysis of model performed by varying different parameters of gasification and the model is validated with experimental data reported in literature [26].

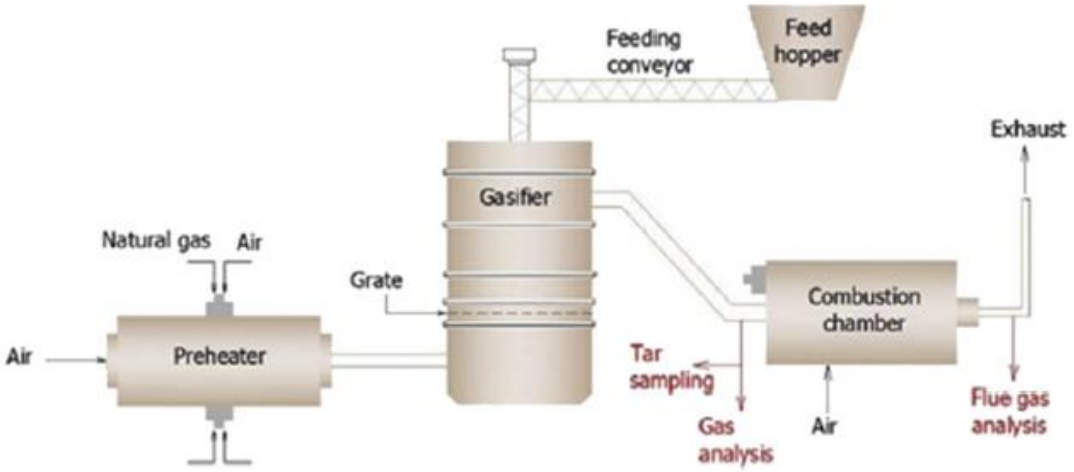

Figure 1.2 : High temperature air gasifier system [26].

Lui et.al 2015, performed the CFD simulation of a pilot-scale biomass gasifier that consisted of a dual fluidized bed to predict the gas composition and syngas temperature. The model is also validated with experimental results [22]. In another study, Silva et.al, 2015, used numerical simulation in the CFD framework to study syngas behavior obtained from three different biomass sources. In contrast, CFD model results were validated under the experimental results data [23]. Tauqir et.al 2019, performed a simulation of downdraft biomass gasification by using Aspen Plus and performed the parametric analysis by adding uncertainty in input variables. The model was developed by using Eq-separate equilibrium method by utilizing the Gibbs free energy minimization technique to approach the equilibrium of biomass gasification reactions [17]. Yang et.al 2019, assessed co-firing biomass gasification with carbon capture storage (CCS) and without CCS and developed a life cycle assessment (LCA) model under the principle of conservation of mass and energy to determine the efficiency of purification devices [27]. Makkawi, et.al, 2019, performed parametric analysis of downer fluidized bed reactor

for biomass pyrolysis reaction. The downer fluidized reactor is implemented in order to separate the gas solid in reactor and increases the residence time of biomass in reactor. It was concluded that pyrolysis temperature is the one who effects the yield [28]. Nugraha et.al 2019, used a simulated model of the biomass gasification process by introducing a particle discretized method (PDM). The numerical accuracy, stability, and efficiency were also tested to know how robust our model predicts gasification processes [24]. Ke, et.al, 2019, developed model for microwave assisted biomass gasifier. It can be used for the prediction of syngas production under unique course of microwave irradiation. In this process, set temperature is achieved in order to perform gasification at set temperature. Microwave irradiation is used by biomass and absorbs, and the internal energy of the systems result in increase of temperature of system [29]. Yang et.al, 2019, used the biomass gasification process at the particle scale level in a fluidized bubbling bed gasifier by using the CFD-DEM coupling method. The three dimensional (3-D) fluidized bed gasifier model is modeled by incorporating species transport model, heat and mass transfer equation, and the model validated using literature. The model presented the vertical distribution of reaction rate and operating parameters in the reactor [30]. Herdem et.al, **2020**, proposed a combined model of biomass gasifier and solar power plants, whereas the simulation of the designed model was carried out using MATLAB®, Aspen Plus® and TRNSYS® [16]. Karim, et.al, 2020, developed numerical model of wood biomass under oxy-fuel conditions. The purpose of this study is to evaluate the performance of reciprocating grate boiler, under oxy-fuel conditions while keeping same thermal load of 3.9 KW. By varying oxy-fuel conditions, it is observed that by increase of O_2, CO_2 is decreased and flame temperature of boiler is increased [31]. Bianco, et.al, 2020, proposed an optimization of biomass feed fired with straw with air manifold. The data of 3D CFD model was analyzed with experimental results. The entropy generation results in many way to improve the an air manifold biomass fired with straw [32]. Sia, et.al, 2020, studied fluidized bed biomass pyrolysis by simulating hydrodynamics and chemical kinetics of biomass by using CFD. The simulation results are validated with experimental data that temperature influences the yield. This study also demonstrates the fluidizing sand and temperature distribution of fluidized gas [33]. Smith, et.al, 2020, designed a biomass

burner using advanced optimization tool. Sculptor is used to identify the behavior of biomass gasification and manipulate the reactor according to environment [34].

Wang, et.al, 2015, performed an exergy analysis of combined cooling heating and power (CCHP) systems to determine the irreversibilities. The heat pipe heat exchanger was installed to recover waste heat from various streams for effective energy utilization during the operation [10]. Karellas et.al, 2016, evaluated the different parameters of the process by performing energy analysis of the cogeneration and tri-generation hybrid simulated system of solar power and biomass fuel and proposed a solution to enhance the system in terms of economic assessment. The sensitivity analysis was performed to estimate the economic effect of biomass and fuels required to operate the system. The observations showed that the reduction in utilities and fuel oil major saving in the capital. [35]. Rahbari et.al, 2018, modeled the solar supercritical water gasification of biomass (SCWG) using Aspen Plus. Then energy analysis is performed to optimize various parameters of the SCWG process [18]. Orrego et.al, 2019, completed the exergy analysis and energy integrated assessment to enhance the biomass gasification process [36]. However, to the best of our knowledge the CFD-based exergy analysis of biomass has not been performed. Nevertheless, Mustafa et.al, 2017, performed an exergy analysis of naphtha reforming reactors by using a novel CFD method. The reaction kinetics were imported through an interface with C- language. The exergy analysis was evaluated based on its profile along the length of reactor [37]. Rehman et.al, 2019, performed an exergy analysis of monolith micro-reactor of SMR using a CFD environment. The CFF algorithm was used to import exergy equations, which helped to evaluate the exergy profile of reactor along its length [2]

1.1 Thesis Outline

The following is a summary of different thesis chapters.

Chapter 2 discusses the biomass gasification process description and reaction mechanism involved during the whole process. This chapter also discusses the process of exergy involved in the gasification process.

Chapter 3 discusses the model development in ANSYS. This chapter discusses the geometry parameters, mesh properties, and cell zone and boundary conditions parameters.

The assumption was made during the process the convergence criterion for a model to be converged.

Chapter 4 discusses the simulation environment in ANSYS. This chapter discusses ANSYS Design Modeler, ANSYS SpaceClaim, ANSYS Mesh, and Ansys Fluent behavior.

Chapter 5 discusses the results and discussion the behavior of different exergies parameters on biomass gasification process.

Summary

Fossil fuels are considered as largest source of power generation. Due to growing demand of power generation fossil fuel cause many environmental impacts like, global warming. That's why there is need to identify a renewable or sustainable source for power generation. Biomass is considered one of the sustainable source of power generation and gain scientists interest.

References

[1] M. A. Chawdhury and K. Mahkamov, "Development of a Small Downdraft Biomass Gasifier for Developing Countries," *J. Sci. Res.*, vol. 3, no. 1, p. 51, 2010.

[2] Z. ur Rahman, I. Ahmad, M. Kano, and J. Mustafa, "Model development and exergy analysis of a microreactor for the steam methane reforming process in a CFD environment," *Entropy*, vol. 21, no. 4, pp. 1–19, 2019.

[3] J. (Universität K. Schmid, *Erneuerbare Energien und Energieeffizienz Renewable Energies and Energy Efficiency*, vol. 14. 2009.

[4] A. Demirbas, "Biofuels from agricultural biomass," *Energy Sources, Part A Recover. Util. Environ. Eff.*, vol. 31, no. 17, pp. 1573–1582, 2009.

[5] K. Kundu, S. Sharma, and T. R. Sreekrishnan, "Influence of Process Parameters on Anaerobic Digestion Microbiome in Bioenergy Production: Towards an Improved Understanding," *Bioenergy Res.*, vol. 10, no. 1, pp. 288–303, 2017.

[6] Y. Chen, H. Liu, X. Zheng, X. Wang, and J. Wu, "New method for enhancement of bioenergy production from municipal organic wastes via regulation of anaerobic fermentation process," *Appl. Energy*, vol. 196, pp. 190–198, 2017.

[7] R. Kleerebezem and M. C. van Loosdrecht, "Mixed culture biotechnology for bioenergy production," *Curr. Opin. Biotechnol.*, vol. 18, no. 3, pp. 207–212, 2007.

[8] M. C. Math, S. P. Kumar, and S. V. Chetty, "Technologies for biodiesel production from used cooking oil - A review," *Energy Sustain. Dev.*, vol. 14, no. 4, pp. 339–345, 2010.

[9] S. Mishra, M. Roy, and K. Mohanty, "Microalgal bioenergy production under zero-waste biorefinery approach: Recent advances and future perspectives," *Bioresour. Technol.*, vol. 292, no. June, p. 122008, 2019.

[10] J. J. Wang, K. Yang, Z. L. Xu, and C. Fu, "Energy and exergy analyses of an integrated CCHP system with biomass air gasification," *Appl. Energy*, vol. 142, pp. 317–327, 2015.

[11] A. Rahbari, M. B. Venkataraman, and J. Pye, "Energy and exergy analysis of concentrated solar supercritical water gasification of algal biomass," *Appl. Energy*, vol. 228, no. June, pp. 1669–1682, 2018.

[12] N. Mazaheri, A. H. Akbarzadeh, E. Madadian, and M. Lefsrud, "Systematic review of research guidelines for numerical simulation of biomass gasification for bioenergy production," *Energy Convers. Manag.*, vol. 183, no. December 2018, pp. 671–688, 2019.

[13] A. Ayub and U. Ibrahim, "Exergy Models and Tar Removal Techniques in Biomass Gasification," *Adv. J. Grad. Res.*, vol. 5, no. 1, pp. 16–23, 2018.

[14] L. Damiani and A. Trucco, "An experimental data based correction method of biomass gasification equilibrium modeling," *J. Sol. Energy Eng. Trans. ASME*, vol. 132, no. 3, pp. 0310111–03101111, 2010.

[15] P. Lü, X. Kong, C. Wu, Z. Yuan, L. Ma, and J. Chang, "Modeling and simulation of biomass air-steam gasification in a fluidized bed," *Front. Chem. Eng. China*, vol. 2, no. 2, pp. 209–213, 2008.

[16] M. S. Herdem, D. Mazzeo, N. Matera, J. Z. Wen, J. Nathwani, and Z. Hong, "Simulation and modeling of a combined biomass gasification-solar photovoltaic hydrogen production system for methanol synthesis via carbon dioxide hydrogenation," *Energy Convers. Manag.*, vol. 219, no. March, p. 113045, 2020.

[17] W. Tauqir, M. Zubair, and H. Nazir, "Parametric analysis of a steady state equilibrium-based biomass gasification model for syngas and biochar production and heat generation," *Energy Convers. Manag.*, vol. 199, no. May, p. 111954, 2019.

[18] A. Rahbari, M. B. Venkataraman, and J. Pye, “Energy and exergy analysis of concentrated solar supercritical water gasification of algal biomass,” *Appl. Energy*, vol. 228, no. July, pp. 1669–1682, 2018.

[19] J. Collazo, J. Porteiro, J. L. Míguez, E. Granada, and M. A. Gómez, “Numerical simulation of a small-scale biomass boiler,” *Energy Convers. Manag.*, vol. 64, pp. 87–96, 2012.

[20] M. A. Gómez, J. Porteiro, D. Patiño, and J. L. Míguez, “CFD modelling of thermal conversion and packed bed compaction in biomass combustion,” *Fuel*, vol. 117, no. PART A, pp. 716–732, 2014.

[21] M. A. Gómez, J. Porteiro, D. Patiño, and J. L. Míguez, “Eulerian CFD modelling for biomass combustion. Transient simulation of an underfeed pellet boiler,” *Energy Convers. Manag.*, vol. 101, pp. 666–680, 2015.

[22] H. Liu, R. J. Cattolica, R. Seiser, and C. hsien Liao, “Three-dimensional full-loop simulation of a dual fluidized-bed biomass gasifier,” *Appl. Energy*, vol. 160, pp. 489–501, 2015.

[23] V. Silva and A. Rouboa, “Combining a 2-D multiphase CFD model with a Response Surface Methodology to optimize the gasification of Portuguese biomasses,” *Energy Convers. Manag.*, vol. 99, pp. 28–40, 2015.

[24] M. G. Nugraha, H. Saptoadi, M. Hidayat, B. Andersson, and R. Andersson, “Particle modelling in biomass combustion using orthogonal collocation,” *Appl. Energy*, vol. 255, no. September, p. 113868, 2019.

[25] S. Barsali, A. De Marco, R. Giglioli, G. Ludovici, and A. Possenti, “Dynamic modelling of biomass power plant using micro gas turbine,” *Renew. Energy*, vol. 80, pp. 806–818, 2015.

[26] T. M. Ismail and M. A. El-Salam, “Numerical and experimental studies on updraft gasifier HTAG,” *Renew. Energy*, vol. 78, pp. 484–497, 2015.

[27] B. Yang, Y. M. Wei, Y. Hou, H. Li, and P. Wang, “Life cycle environmental impact assessment of fuel mix-based biomass co-firing plants with CO2 capture and

storage," *Appl. Energy*, vol. 252, no. June, p. 113483, 2019.

[28] Y. Makkawi, X. Yu, and R. Ocone, "Parametric analysis of biomass fast pyrolysis in a downer fl uidized bed reactor," vol. 143, pp. 1225–1234, 2019.

[29] C. Ke *et al.*, "Syngas production from microwave-assisted air gasification of biomass: Part 1 model development," *Renew. Energy*, vol. 140, pp. 772–778, 2019.

[30] S. Yang, H. Wang, Y. Wei, J. Hu, and J. W. Chew, "Particle-scale modeling of biomass gasification in the three-dimensional bubbling fluidized bed," *Energy Convers. Manag.*, vol. 196, no. May, pp. 1–17, 2019.

[31] M. R. Karim, A. A. Bhuiyan, A. A. R. Sarhan, and J. Naser, "CFD simulation of biomass thermal conversion under air/oxy-fuel conditions in a reciprocating grate boiler," *Renew. Energy*, vol. 146, pp. 1416–1428, 2020.

[32] V. Bianco, M. Szubel, B. Matras, M. Filipowicz, K. Papis, and S. Podlasek, "CFD analysis and design optimization of an air manifold for a biomass boiler," *Renew. Energy*, vol. 163, pp. 2018–2028, 2021.

[33] S. Q. Sia and W. C. Wang, "Numerical simulations of fluidized bed fast pyrolysis of biomass through computational fluid dynamics," *Renew. Energy*, vol. 155, pp. 248–256, 2020.

[34] J. D. Smith, V. Sreedharan, M. Landon, and Z. P. Smith, "Advanced design optimization of combustion equipment for biomass combustion," *Renew. Energy*, vol. 145, pp. 1597–1607, 2020.

[35] S. Karellas and K. Braimakis, "Energy-exergy analysis and economic investigation of a cogeneration and trigeneration ORC-VCC hybrid system utilizing biomass fuel and solar power," *Energy Convers. Manag.*, vol. 107, pp. 103–113, 2016.

[36] D. Flórez-Orrego, F. Maréchal, and S. de Oliveira Junior, "Comparative exergy and economic assessment of fossil and biomass-based routes for ammonia production," *Energy Convers. Manag.*, vol. 194, no. April, pp. 22–36, 2019.

[37] J. Mustafa, I. Ahmad, M. Ahsan, and M. Kano, "Computational fluid dynamics

based model development and exergy analysis of naphtha reforming reactors," *Int. J. Exergy*, vol. 24, no. 2–4, pp. 344–363, 2017.

Chapter 2: Theoretical Background

2.1 Process Description

A biomass gasifier is used for the partial combustion (gasification) of solid fuel (biomass) at a temperature of up to 1300^0C. Biomass gasification is the thermal conversion of solid biomass to volatile combustible products i.e. carbon monoxide (CO), Hydrogen (H_2), and methane (CH_4) [1]. There are also some by products like tar and dust. These products are produced by the reaction of carbon dioxide and water in the occurrence of charcoal. The gasifier is designed at such conditions that maximum combustible gases are produced like producer gas, biogas, and carbon dioxide.

Gasifiers are classified into various types, depends upon the type of feed introduced into the gasifier. In a downdraft gasifier, biomass feedstock travels in a downwards direction.

Gasification is divided into four distinct processes, i.e. drying, pyrolysis, oxidation, and reduction, shown in Figure 2.1 [1], [2].

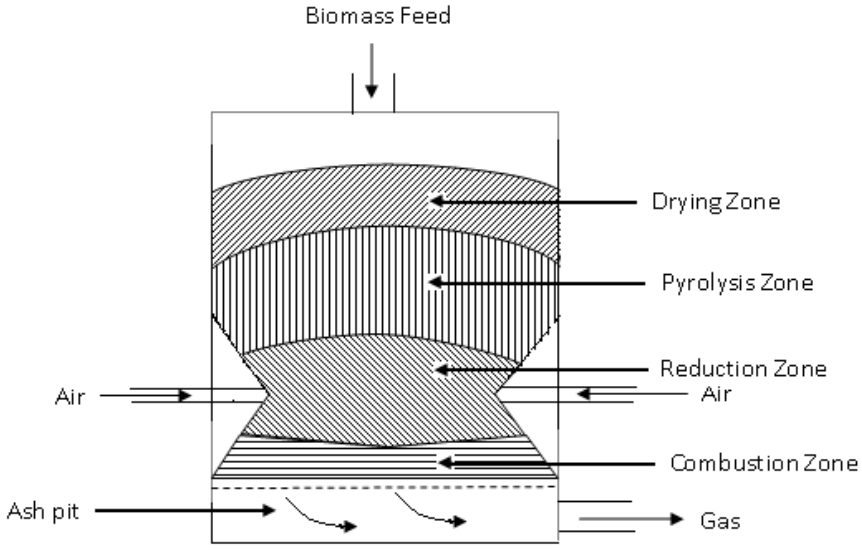

Figure 2.1: Downdraft biomass gasifier [2]

The first step in gasification is drying, in which moisture is evaporated by adding a specific amount of heat. The second step is pyrolysis, which is the thermal conversion of biomass into a lower weight compound. Pyrolysis reaction occurs at around 300^0C, where solid

biomass is converted into char (C), and volatile components. In the third step biomass is oxidized to generate energy for the upcoming endothermic processes, i.e, reduction reactions. In the fourth step where reduction reaction happens, gas mixture and char react to form syngas (CO, H_2) [3].

The reaction mechanisms of biomass gasification are summarized in Table 2.1.

Table 2.1: Elementary reactions for Biomass Gasification

S.No.	Mechanism	Reaction
1	Pyrolysis	$Biomass_{(aq)}$ –> $H_2O_{(l)}$ + 0.268 CO + 0.295 CO_2 + 0.094 CH_4 + ASH + 0.5H_2+ 0.255 $H_2O_{(g)}$ + 0.004 NH_3 + 0.0002 H_2S + 0.2 P-Tar + Char
2	Drying	$H_2O_{(l)}$ –> $H_2O_{(g)}$
3	Tar Cracking	P-Tar –> 0.261 S-Tar + 2.6 CO + 0.441 CO_2 + 0.983 CH_4 + 2.161 H_2 + 0.408 C_2H_4
4	Char decomposition	$2C_{(s)}$ + O_2 –> 2CO
5		$C_{(s)}$ +O_2 –> CO_2
6		$C_{(s)}$ + H_2O –> CO + H_2
7		$C_{(s)}$ + CO_2 –> 2 CO
8	Homogeneous reaction	P-Tar + O_2 –> H_2O + CO
9		S-Tar + O_2 –> H_2O + CO
10		H_2 + 0.5 O_2 –> H_2O
11		CO + 0.5 O_2 –> CO_2
12		CO + H_2O –> H_2 + CO_2
13		CH_4 + 1.5 O_2 –> CO + 2H_2O
14		CH_4 + H_2O –> CO + 4H_2

2.2 Process Exergy

Zoran Rant introduced the term exergy, which means the work (-erg) that has been released (ex-) [4]. Exergy can be stated as;

"The maximum useful work that can be obtained from an energy carrier when it is brought from the initial state to a state of equilibrium with the environment (dead state) due to the irreversibilities in processes". [5], [6].

Exergy can also be represented by the quality of energy, as it is only possible to work that can be obtained from the system. The entropy means the energy losses of the system due

to irreversibilities. The second law of thermodynamics defines a relation between entropy and exergy. Entropy production is exergy degradation in actual process equipment or exergy losses during entire processes.

2.2.1 Components of Process Exergy:

The total exergy of a system is the summation of chemical, physical and mixing exergy is shown in Equation 1:

$$E = E^{ph} + E^{\Delta mix} + E^{ch} \quad (1)$$

where the total molar exergy of a system is represented by E, the molar physical exergy is represented by E^{ph}, E^{mix} represents the molar mixture exergy and the molar chemical exergy is represented by E^{ch} [4].

The physical exergy is the maximum obtainable work, when the system is brought from actual conditions (T, P) to thermomechanical equilibrium at ambient temperature (T0, P0) by the reversible process.

The following equations give a generalized representation of the molar physical exergy.

$$E^{ph} = RT_o \sum_{i=1}^{n} ln\frac{p_i}{p_o} + \sum_{i=1}^{n} C_{p_i}^{mean}(T_i - T_o - T_o ln(\frac{T_i}{T_o})) \quad (2)$$

$$C_{p_i}^{mean} = \int_{T_1}^{T_2} C_{p_i} \Delta T \quad (3)$$

$$C_{p_i}(\frac{j}{K.mol}) = a_i + b_i T + C_i T^2 + d_i T^3 \quad (4)$$

Where, heat capacity coefficients are a_i, b_i, c_i, and d_i and the ideal gas constant is R [4]. T_i and P_i represent component's temperature and partial pressure, respectively [6].

Similarly, the maximum obtainable work when a material stream moves from thermomechanical equilibrium to chemical equilibrium is knows as chemical exergy[6].The following equations give a generalized representation of the molar chemical exergy.

$$E^{ch} = \sum_{i=1}^{n} v_i \tilde{G}_i(Reactants) + \sum_{i=1}^{n} v_i \tilde{G}_i(Products) \quad (5)$$

$$\tilde{G}_i = G_f^0 + [\tilde{G}_{i(T,P)} - \tilde{G}_{i(T_0,P_0)}] \quad (6)$$

Where v_i, is the stoichiometric coefficient, $\tilde{G}_i$ is the molar Gibbs free energy of component i, and G^0_f is the molar Gibbs free energy of formation [7].

The mixing exergy is the maximum obtainable work from a material stream, when mixing pure components occurs isobariclly and isothermally [8]. The following equations give a generalized representation of the molar mixing exergy.

$$E^{mix} = \sum_{i=1}^{n} x_i T_o R ln x_i \quad (7)$$

Where, x_i is a mass fraction of component *i*. Mixing exergy is always decreasing because the mixing of different components lowers the exergy continuously [4]. The mixing exergy can also be written in the form of $\sum_{i=1}^{n} \frac{x_i R T_o ln p_i}{p_o}$, where P_i is the partial pressure of component i, ($P_i = X_i P_{total}$) according to Dalton's law [9].

Summary

Biomass gasification is the thermochemical conversion of biomass into volatile gases. The biomass gasification process are divided into four steps, drying, pyrolysis, combustion, and decomposition. The Exergy analysis of system is total amount useful work obtained from system. The exergy analysis is summation of three types of exergies, physical exergy, chemical exergy, mixing exergy.

References:

[1] R. R. Kumar, M. N. Baba, K. S. Kumar, and A. V. Vishnu, "Cfd Simulation of Down Drought Biomass Gasifier," *Int. J. Adv. Eng. Res. Dev.*, vol. 3, no. 01, pp. 58–64, 2016.

[2] W. Tauqir, M. Zubair, and H. Nazir, "Parametric analysis of a steady state equilibrium-based biomass gasification model for syngas and biochar production and heat generation," *Energy Convers. Manag.*, vol. 199, no. May, p. 111954, 2019.

[3] M. Trninic, D. Stojiljkovic, A. Jovovic, and G. Jankes, "Biomass gasification technology: The state of the art overview," *4th Int. Symp. Environ. Friendly Energies Appl. EFEA 2016*, 2016.

[4] N. Sato, *Chemical energy and exergy: An introduction to chemical thermodynamics for engineers*, 1st Editio. Elsevier Science, 2004.

[5] F. C. Krysiak, "Management as a Tool for Sustainability," vol. 85, no. 2009, pp. 483–492, 2013.

[6] J. Mustafa, I. Ahmad, M. Ahsan, and M. Kano, "Computational fluid dynamics based model development and exergy analysis of naphtha reforming reactors," *Int. J. Exergy*, vol. 24, no. 2–4, pp. 344–363, 2017.

[7] M. B. B. Michael J. Moran, Howard N. Shapiro, Daisie D. Boettner, *Fundamentals of Engineering Thermodynamics*, 9th ed. Wiley, 2018.

[8] A. P. Hinderink, F. P. J. M. Kerkhof, A. B. K. Lie, H. J. V. A. N. D. E. R. Kooi, and P. Equilibria, “SIMULATOR--I . THEORY ; CALCULATING EXERGIES OF,” vol. 51, no. 20, 1996.

[9] A. Plus, A. Plus, A. Plus, and A. Plus, “Use of MHBT for the Practical Case,” pp. 81–84, 2013.

Chapter 3: Model Development

Computational fluid dynamics (CFD) is the science that defines the phenomena of fluid flow, mass transfer, heat transfer, and all related mechanisms, by solving through mathematical models. To solve these mathematical models computing systems must evaluate the interfaces between gases and liquid surfaces described by boundary conditions. Various software is developed to simulate these mathematical models, ANSYS, Aspen, and MATLAB are a few of them. These software helps in the design of processes, detailed study of process equipment and redesigning of process.

3.1 Assumptions

The CFD based model development requires certain assumptions. These are as follows:

1. The system achieved an equilibrium state and maximum yield can be achieved
2. The reactor wall is well isolated. So there is negligible heat loss to the environment
3. The laminar flow is assumed and the process takes place in steady state conditions
4. The gas mixture is considered an ideal gas and incompressible

3.2 Geometry and Meshing

ANSYS Design Modeler® and Space Claim® was used to create the geometry of downdraft biomass gasification. The lab-scale model of the gasifier is the design and the height of reactor is 1.751m. ANSYS Mesh® was used to define the mesh of the gasifier reactor as shown in Figure 3.1.

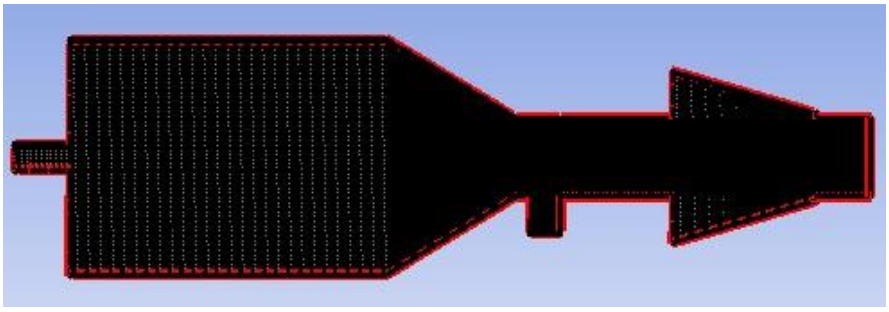

Figure 3.1: Mesh of biomass gasifier

The mesh properties were adopted was shown in Table 3.1. The number of nodes, number of cells, orthogonal quality, ortho skew, aspect ratio, and surface area, was 50514, 49971, 0.99, 0.003, 1.67 and 0.53 m^2, respectively.

Table 3.1: Mesh properties

Properties of Mesh	Values
Orthogonal quality (average)	0.99
Ortho skew (average)	0.003
Aspect ratio (average)	1.67
The number of nodes	50514
The number of cells	49971
Surface area (m^2)	0.53

3.3 Boundary and Cell Zone Conditions

The inlet and outlet boundary conditions for the downdraft biomass gasifier was shown in Table 3.2. The ratio of inlet composition of biomass mixture with air was set to 1: 6.5. The wall of the reactor is kept isothermal. It favors the formation of H_2 fuel from biomass and air-steam through highly exothermic reactions. The flow regime is a continuum, and on the walls of the gasifier the no-slip condition is used.

Table 3.2: Model Parameters

Parameter	Values
Channel length	1.751 m
Inlet temperature	298.16 K
Isothermal wall temperature	298.16 K
Pressure Outlet	102325 pa
Inlet mass flow	100 kg/s
Ratio of Biomass to air	0.22

3.4 CFD Conservative Equations

The discretization of the species transport equation, continuity equation, energy equation, and momentum equation can be occurred by using finite volume methods with the help of cell centered configuration. Conservation laws are applicable to each control volume by

using the above fundamental equations. A planar steady-state model is formed by integrating it with the heterogeneous and homogeneous reaction schemes of biomass gasification.

2.4.1 Species Transport Equation

$$\frac{\partial \rho Y_i}{\partial t} + \frac{\partial \rho u_x Y_i}{\partial x} + \frac{\partial \rho u_y Y_i}{\partial y} = -[\frac{\partial j_{i,x}}{\partial x} + \frac{\partial j_{i,y}}{\partial y}] + \dot{S}_i \quad (3.1)$$

$$j_{i,x} = -\rho D_i \frac{\partial Y_i}{\partial x} \quad (3.2)$$

$$j_{i,y} = -\rho D_i \frac{\partial Y_i}{\partial y} \quad (3.3)$$

Where, the mass fraction of component i is Y_i, diffusion coefficient is D_i, mass flux of component I J_i, and the net production rate is $\dot{S}_i$ of species through chemical reactions [1].

2.4.2 Energy Conservative Equation

$$\rho \frac{\mathrm{de}}{\mathrm{dt}} = -\mathrm{P}\ \mathrm{div}\ \mathrm{u} + \mathrm{div}\ (\mathrm{k}\ \mathrm{grad}\ \mathrm{T}) + \Phi + \mathrm{S} \quad (3.4)$$

$$div\ u = \frac{\partial u_x}{\partial x} + \frac{\partial u_y}{\partial y} \quad (3.5)$$

$$gradT = \frac{\partial T}{\partial x} + \frac{\partial T}{\partial y} \quad (3.6)$$

$$i = C_v T \quad (3.7)$$

$$P = \rho RT \quad (3.8)$$

$$\phi = \mu\{2[(\frac{\partial u_x}{\partial x})^2 + (\frac{\partial u_y}{\partial y})^2] + (\frac{\partial u}{\partial y} + \frac{\partial v}{\partial x})^2\} \quad (3.9)$$

Where, e is the specific internal energy, C_v is the specific heat constant, and k is the thermal conductivity. ϕ shows the rate of dissipation energy per unit volume and S denotes the work done per unit volume by body forces. The first term of the right-hand side of Equation (3.4) is the rate of work done per unit volume, and the second term is the rate of heat transfer per unit volume through conduction [2].

2.4.3 Continuity Equation

$$\frac{\partial \rho}{\partial t} + \frac{\partial (\rho u_x)}{\partial x} + \frac{\partial (\rho u_y)}{\partial y} = S_m \quad (3.10)$$

Where $\rho, u_x, and\ u_y$ are the density, velocity in x, and y-direction respectively. *Sm* represents a mass addition to the continuous phase which is zero in this case. The first term of the LHS of the equation shows the change of density per unit time local derivative at the fixed point. The second and third terms show density of the gas mixture convective derivative [3].

2.4.4 Momentum Equations

$$\frac{\partial(\rho u_x)}{\partial t} + \frac{\partial(\rho u_x u_x)}{\partial x} + \frac{\partial(\rho u_x u_y)}{\partial y} = -\frac{\partial P}{\partial x} + \frac{\partial}{\partial x}[\frac{4}{3}\mu\frac{\partial u_x}{\partial x} - \frac{2}{3}\mu\frac{\partial u_y}{\partial y}] + \frac{\partial}{\partial y}[\mu(\frac{\partial u_y}{\partial x} + \frac{\partial u_x}{\partial y})] \quad (3.11)$$

$$\frac{\partial(\rho u_y)}{\partial t} + \frac{\partial(\rho u_y u_x)}{\partial x} + \frac{\partial(\rho u_y u_y)}{\partial y} = -\frac{\partial P}{\partial y} + \frac{\partial}{\partial y}[\frac{4}{3}\mu\frac{\partial u_y}{\partial y} - \frac{2}{3}\mu\frac{\partial u_x}{\partial x}] + \frac{\partial}{\partial x}[\mu(\frac{\partial u_y}{\partial x} + \frac{\partial u_x}{\partial y})] \quad (3.12)$$

Where, stream pressure is represented by P and viscosity of the gas stream is represented by μ. The 1st term of the RHS of each equation shows pressure P forces. The 2nd and 3rd terms of each equation's show the viscous μ forces [1].

3.5 Chemical Reactions:

The chemical reactions involved in biomass gasification is shown in Chapter 2. The first mechanism is of pyrolysis, when biomass is fed into gasifier, the biomass decomposes to char, volatile components, ash and tar. Basically, the volatile matters consists of CO, CO_2, CH_4, etc.

Biomass (aq) –> H_2O (l) + 0.268 CO + 0.295 CO_2 + 0.094 CH_4 + ASH + 0.5H_2+ 0.255 H_2O (g) + 0.004 NH_3 + 0.0002 H_2S + 0.2 P-Tar + Char (3.13)

The second step is drying, in which moisture is evaporated by adding heat to the system. The heat released during pyrolysis is used for the drying process. To maintain the system energy efficient.

H_2O (l) –> H_2O (g) (3.14)

Then afterwards, tar cracking is take place in which primary tar is converted into volatile components and secondary tar. For cracking of tar around 900°C temperature is required.

P-Tar –> 0.261S-Tar + 2.6 CO + 0.441 CO_2 + 0.983 CH_4 + 2.161 H_2 + 0.408 C_2H_4 (3.15)

For good tar cracking, around 1300K temperature is required to maintain the process sustainable. After tar cracking char decomposition occurred, in which char is converted to volatile matters. After char conversion, combustion takes place in which final products are obtained. This is exothermic reaction in which heat is evolved sometimes flame temperature exceeds the 2000^0C. The reactions involved in char decomposition and combustion are shown in Table 2.1.

3.6 Computational Scheme

A schematic flowchart of our computational model is shown in Figure 3.2. Firstly, the geometry of the gasifier was developed followed by mesh preparation. Then, boundary and cell zone conditions were identified. The mesh file was imported to ANSYS Fluent simulator. To evaluate the temperature effects, the energy equation was kept on as temperature variation occurs during reaction. The reaction mechanism was imported using the species transport model. Fluent 16.0 was used to numerically solve the governing equations i.e., continuity, energy, and species conservation. The mathematical model was discretized by using a second-order upwind scheme. The SIMPLE algorithm scheme was used for velocity-pressure coupling. To slow down the rate of change, an under-relaxation factor was used. The eddy dissipation model calculated the rate of reaction. The CFF algorithm was used to perform the exergy analysis. The convergence depends on the residuals of all governing equations involved in CFD simulations. The number of iterations required to converg all governing equations in our CFD model was 827, as shown in Figure 3.3.

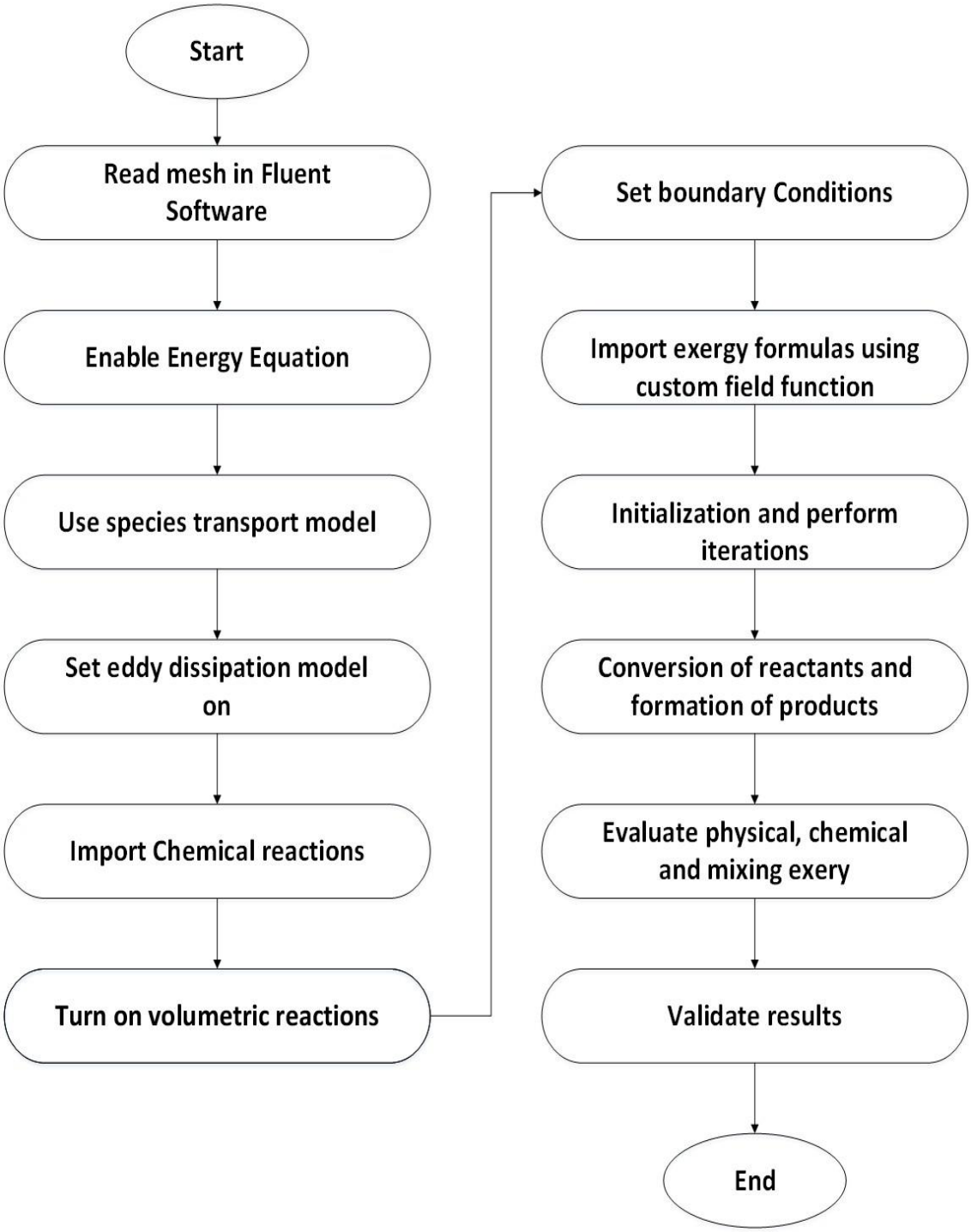

Figure 3.2: Schematic chart of our computational model

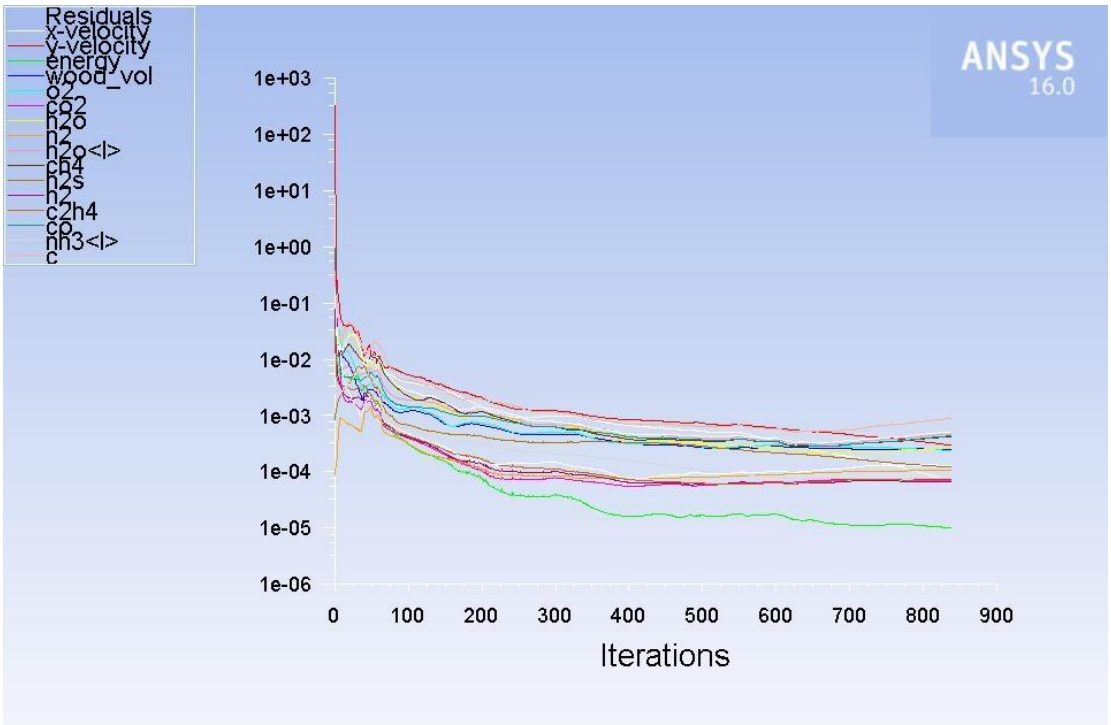

Figure *3.3*: Converging residuals of our model

Summary

The CFD based model of biomass gasifier is developed. Ansys is used for the compuational model development. The reaction mechanism was imported using using species transport model. The SIMPLE algorithm is used for velocity pressure coupling. The rate of reaction was calculated using eddy dissipation model. The CFF algorithm is used to import exergy equations.

References

[1] C. Cao, N. Zhang, X. Chen, and Y. Cheng, "A comparative study of Rh and Ni coated microchannel reactor for steam methane reforming using CFD with detailed chemistry," *Chem. Eng. Sci.*, vol. 137, pp. 276–286, 2015.

[2] F. Moukalled, L. Mangani, M. Darwish, and others, *The finite volume method in computational fluid dynamics*, vol. 6. Springer, 2016.

[3] K. G. Menon and V. S. Patnaikuni, "CFD simulation of fuel reactor for chemical looping combustion of Indian coal," *Fuel*, vol. 203, pp. 90–101, 2017.

Chapter 4: Simulation Environment

4.1 Model Design

Design modeler is one of the tools used for making geometry. Design modelers are very basic and user-friendly compared to other tools like, AutoCAD, Gambit, etc. In this work, a two dimensional lab scale biomass gasifier geometry was developed using vertices. Edges were formed by connecting these vertices, which can be converted into faces later on. The design modeler GUI is shown in Appendix B Figure 4.1.

Space Claim was used to define the faces on geometry developed by the design modeler. The vertices and edges formed previously are used to make faces. Appendix B Figure 4.2 shows how edges and vertices are combined in order to form different faces.

3.1.1 Design Parameters

The boundary box for the design model is shown in Table 4.1. The design biomass gasifier have an area of 0.52735 m^2.

Table 4.1: Bounding Box for design model

Length	Geometry
X-axis	0.45743 m
Y-axis	1.751 m

4.2 Mesh

The meshing of designed geometry in the design modeler and space claim was done in ANSYS Mesh. Figure 4.1 shows the meshed downdraft biomass gasifier. When meshing of geometry is completed, then boundary walls, inlet and outlet, and interior surface of geometry was assigned is shown in Appendix B Figure 4.3. The properties of mesh are shown in the section of meshing. The interface for ANSYS Mesh is shown in Appendix B Figure 4.4.

3.2.1 Mesh properties

The mesh properties of downdraft biomass gasifier is shown in Table 4.2.

Table 4.2: Statistics of Mesh

Properties	Statistics
Nodes	50514
Elements	49791
Mesh Metric	
Aspect Ratio	0.62342
Element Quality	0.99897
Jacobian Ratio	1.0033
Parallel Deviation	0.14056
Warping Factor	0
Inflation	
Inflation Option	Smooth Transition
Transition Ratio	0.272
Sizing	
Min face Size	0.0054739 m
Max face Size	0.027369 m

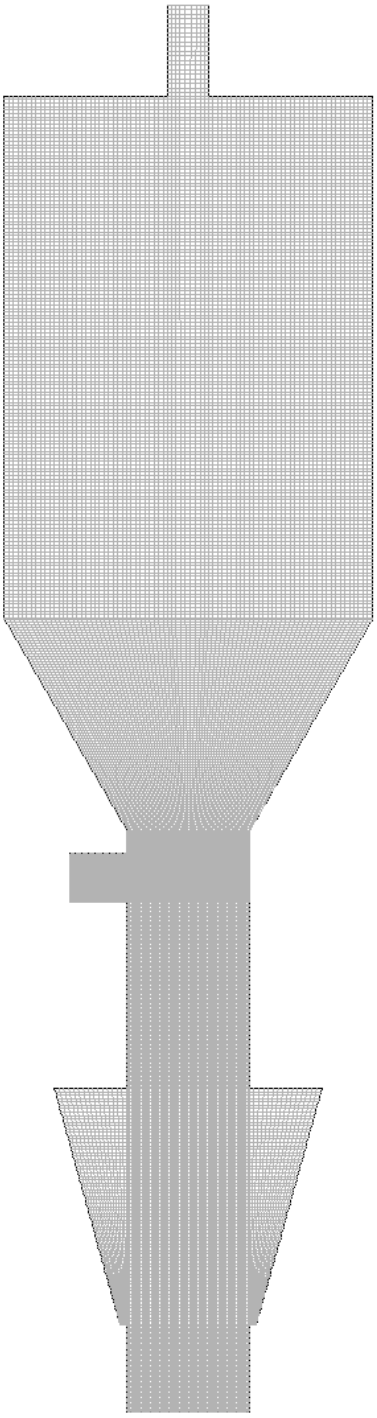

Figure 4.1: Mesh of downdraft biomass gasifier

4.3 Model Simulation

The meshed geometry from ANSYS Mesh is now imported to ANSYS Fluent for further simulation. The species transport, energy and mass conservative equation was solved using finite control volume methods. The quality of the mesh was calculated in fluent. In Fluent, the boundary and zone conditions were specified. The pressure-velocity based solver method was chosen under solution methods. Under the models section, the energy equation was kept on, and the k-epsilon viscous model was selected. The species transport model was selected in order to add the material mixture of wood-volatile air as shown in Appendix B Figure 4.5. After selecting the material mixture the reaction mechanism was imported for biomass gasifier by adding reactions one by one which is shown in Appendix B Figure 4.6. While, under turbulence chemistry interactions, there are four different models to dealt with reactions during the process. The Eddy-dissipation reaction model was chosen among these four models. In this model, reaction rate was controlled and determined by turbulence created during the reaction. The values required to setup the reaction schema are a stoichiometric factor, rate exponent, mixing rate, and activation energy. Figure 4.7 and 4.8 (Appendix B) represent the turbulence chemistry interaction model and the parameters required to import reaction schema.

4.4 Custom Field Function

ANSYS Fluent is used for the analysis of fluid flow dynamics. In order to solve chemical processes, custom coding is required through an external interface. A custom Field Function (CFF) is used to incorporate the energy analysis formulas. Figure 4.9 and 4.10 (Appendix B) shows the CFF calculator and defined field functions.

4.5 Convergence Criterion

The most common convergence criteria used for continuity, species and velocity models are 0.001, while the criteria for energy equations are 0.00001. Figure 4.11 (Appendix B) shows the residual monitor settings. The absolute solution for my model is converged in 827 iterations as shown in chapter 3.

4.6 Experimental Matrix:

The number of experiments were performed in order to obtained best results. The results obtained during these experiments is shown in Table 4.3 and Figure 4.2 and 4.3.

Table 4.3: Experimental Matrix

S.No	Elements Div.	Mole fraction of CO_2	Temperature
1	49.791k	2.47E-1	1.27E3 K
2	11.513k	4.04E-1	9.07E3 K
3	7.987k	4.09E-1	1.14E3 K

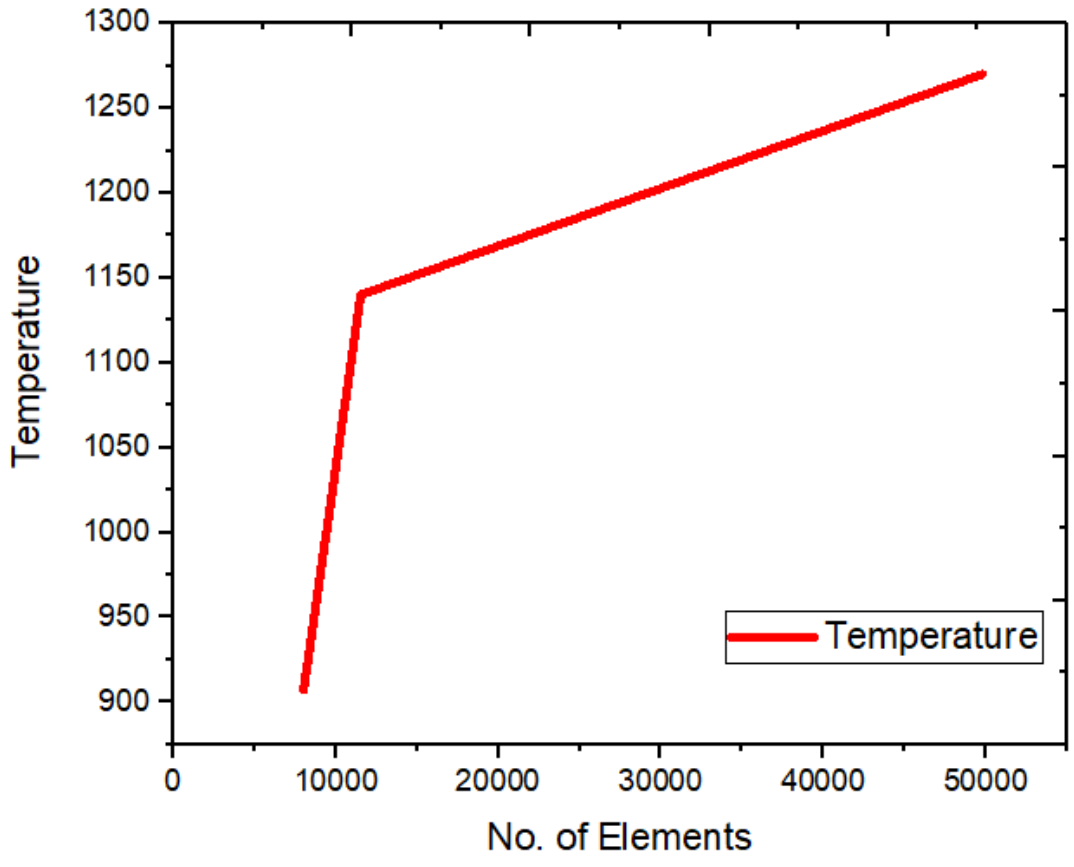

Figure 4.2: No. of elements vs Temperature

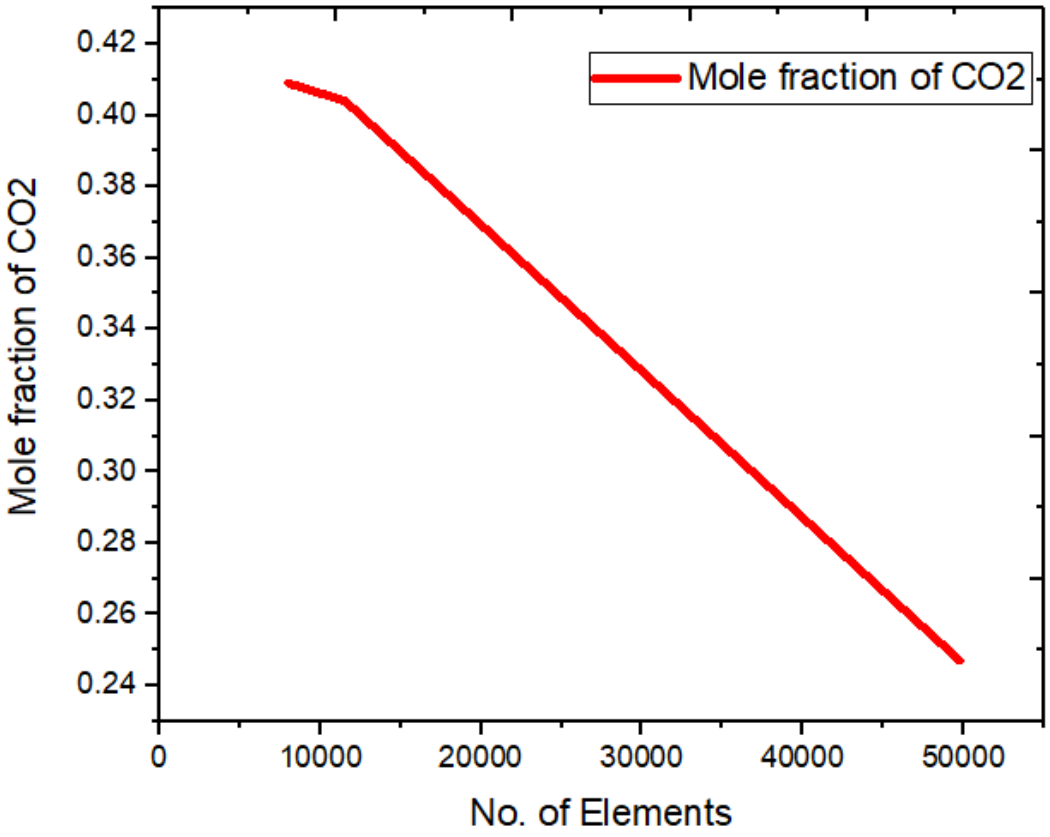

Figure 4.3: No. of elements vs Mole fraction of carbon dioxide

Summary

The simulation environment of biomass gasification in CFD consist of following steps, geometry development using design modeler, and space claim, meshing was done by using Ansys Mesh, then model simulation was carried out by using Ansys fluent. Then, CFF was used to import exergy codes.

Chapter 5: Results and Discussion

The result and discussion are divided into three subsections, i.e., physical properties, reactants and product concentration, and exergy analysis.

Table 5.1: Comparison of the proposed model with literature

Parameter	Simulated data	Literature data
Feed Temperature	298 K	298 K
Combustion temperature	1100 K	800 - 1000K
Ratio of syngas	1.55	1.50

5.1 Physical Properties

The temperature contours and graphs are shown in Figure 1 and 2, respectively, represent the variation in temperature as the reaction happens. Due to some highly exothermic reactions, the reactor temperature is high and uses heat for endothermic reactions. The gasification temperature reported in the literature was up to 1000 K, while in our model, the gasification temperature was up to 1100 K[1], [2]. The composition of CO and H_2 increased due to increased temperature [3]. It is reported that a high temperature is required to produce of more combustible gases during the gasification process [4]. In another study, it is reported that a higher gasification temperature is required for tar cracking processes [5]. The increased temperature of the gasifier also results in higher exergy efficiencies [6].

Pressure contour and graph are shown in Figure 5.1 and 5.3, respectively. As the reaction proceeds the pressure starts decreasing, due to increasing fluid velocity across the reactor. The Bernoulli equation demonstrates this decreasing trend of pressure as velocity increases. In a study performed by zia, et.al, 2019, similar trend is obtained while performing an exergy analysis of steam methane reforming using CFD [7].

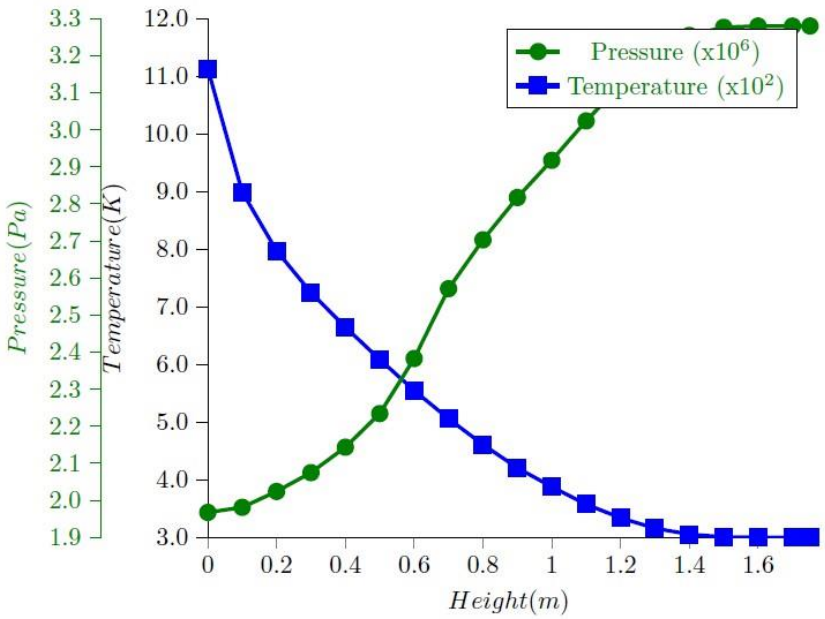

Figure 5.1: Temperature and Pressure profile along height of reactor

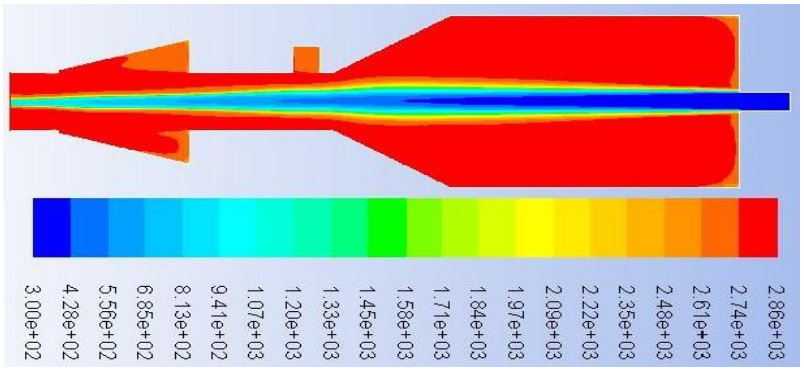

Figure 5.2: Contour of temperature

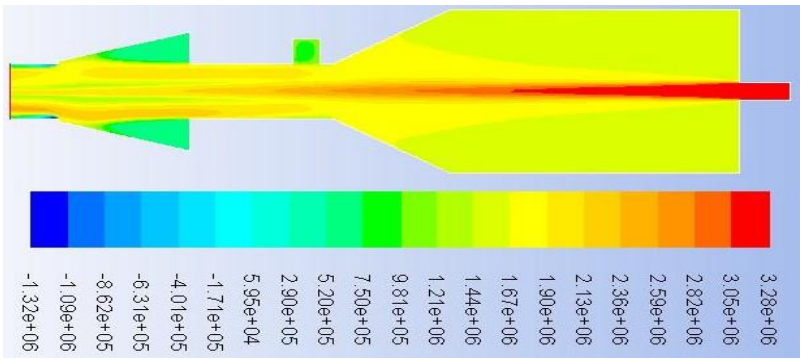

Figure 5.3: Contour of pressure

5.2 Reactants and Products Concentration

The contours and graph of volatile wood are shown in Figures 5.4 and 5.5, respectively. The mole fraction of wood starts decreasing from .133 to 0.098. Table 1 shows the simulated model comparison with data reported by Luo, et.al, 2018 [1]. The simulated model achieved a better syngas ratio of 1.55:1 as carbon monoxide production is increased due to higher gasification temperature. In another study, Jun, et.al, 2017, performed a simulation of downdraft biomass gasification and achieved a syngas ration of 1.14:1 which is much lesser than our model [8].

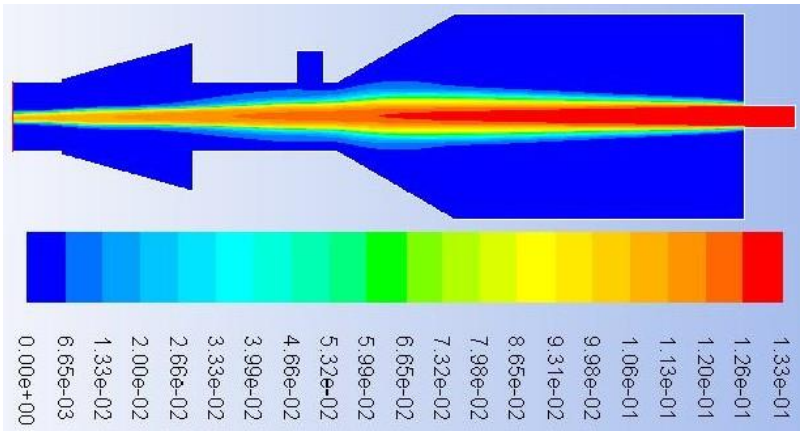

Figure 5.4: Contours of Wood

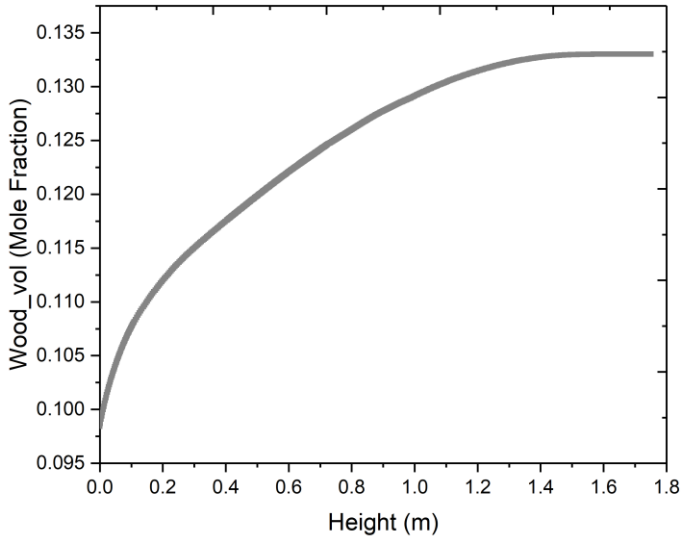

Figure 5.5: Mole fraction of wood along height of reactor

Figures 5.6 and 5.7 show the contours and graphical representation of oxygen present in the reactor. The mole fraction of oxygen in the reactor lies in the range of 0 to 0.18. Oxygen composition decreases along with the depth of the reactor as the reaction takes place. When the reaction takes place oxygen reacts with carbon to form carbon monoxide and carbon dioxide. That's why the mole fraction of oxygen drops from 0.182 to 0.118.

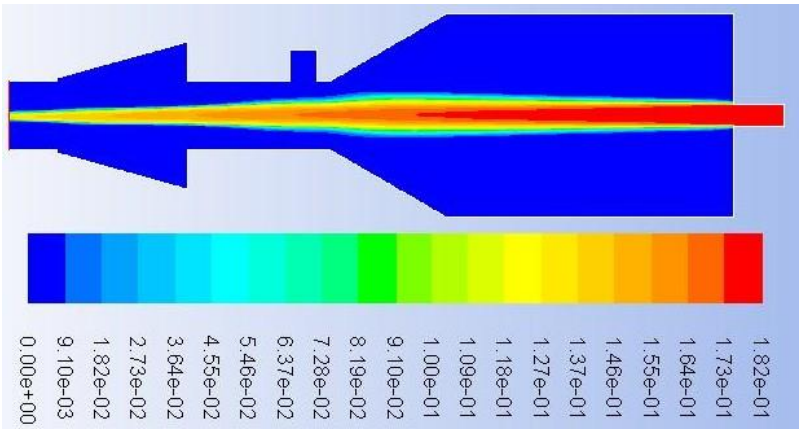

Figure 5.6: Contours of Oxygen

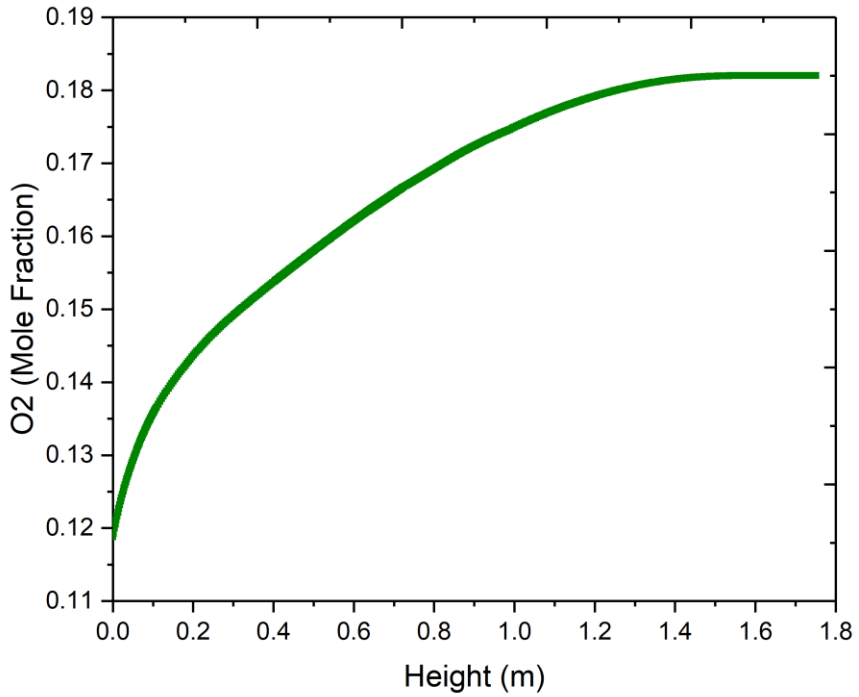

Figure 5.7: Oxygen profile along with the height of reactor

The graph and contour of mole fraction of carbon monoxide are shown in Figures 5.8 and 5.9. Carbon monoxide (CO) forms in primary pyrolysis where the volatile matter is converted into gases. The CO composition is from 0 to 0.03184 inside the reactor, while it increases along with the depth of the reactor. The increasing temperature of the gasifier also causes an increase in the concentration of carbon monoxide in reactor.

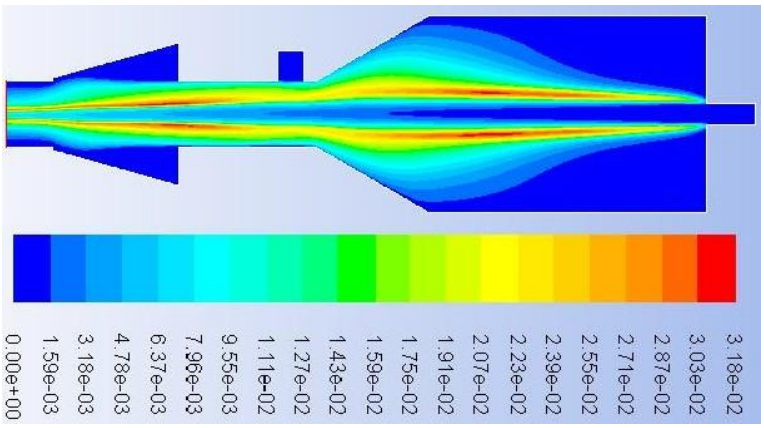

Figure 5.8: Contours of carbon monoxide

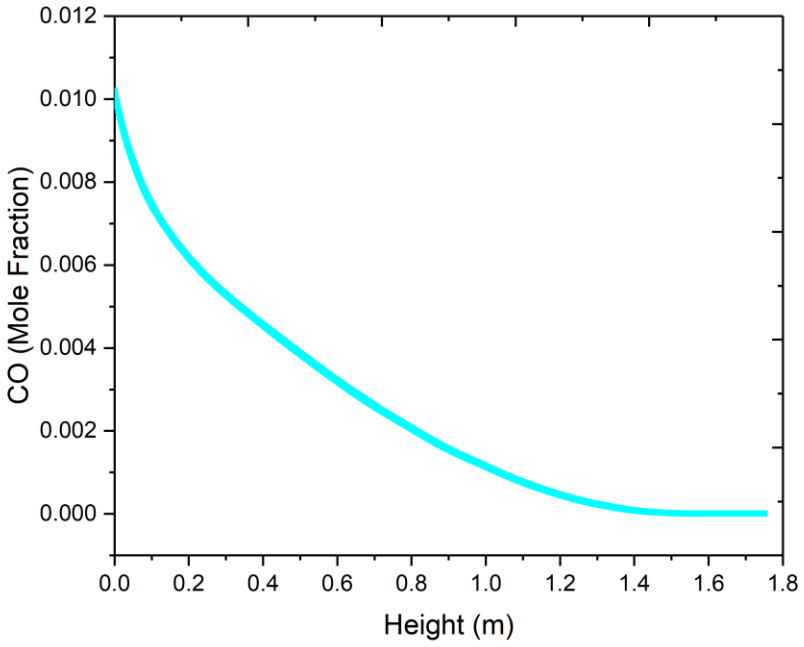

Figure 5.9: Carbon monoxide profile along with the height of the reactor

The contours and graphical representation of carbon dioxide are shown in Figures 5.10 and 5.11, respectively. The carbon dioxide (CO_2) mole fraction is from 0 to 0.247 inside the reactor, whereas the reactor's depth increases. As the reaction proceeds forward, the carbon monoxide and oxygen react to produce carbon dioxide and homogeneous reaction

like, water gas shift reaction also results in the formation of carbon dioxide. Rupesh, et.al, 2016, performed an Aspen PLUS simulation of air-steam biomass gasification, and found that beyond 1000 K temperature the maximum composition of CO_2 was obtained. The sorbent CaO was used to reduce the composition of CO_2 and maximize the production of hydrogen gas [9].

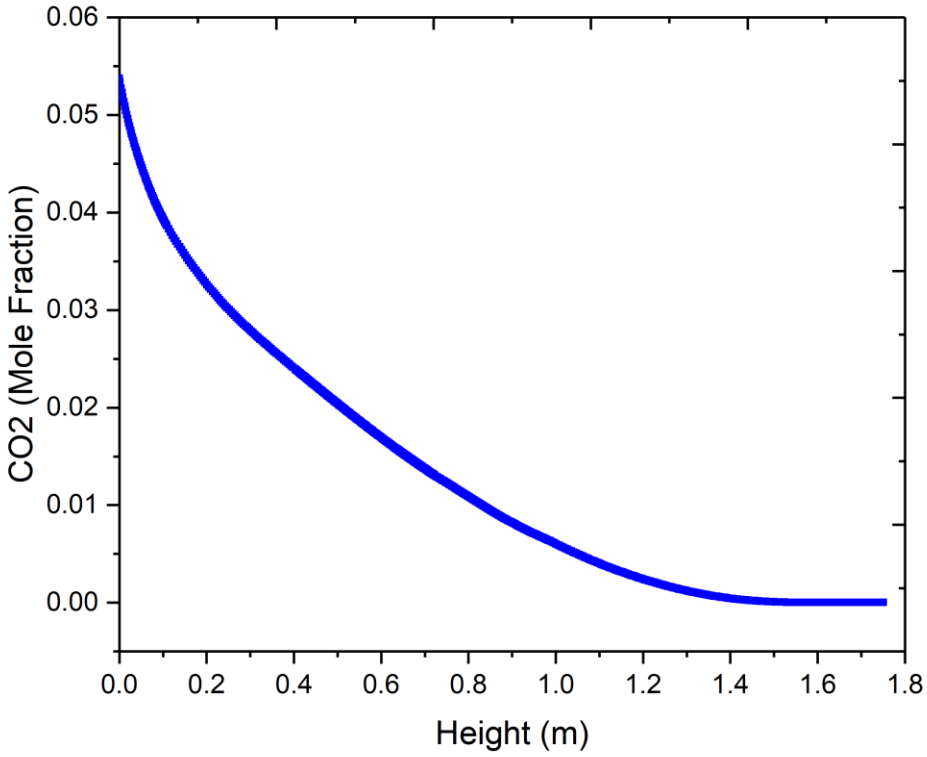

Figure 5.10: Carbon dioxide profile along with the height of the reactor

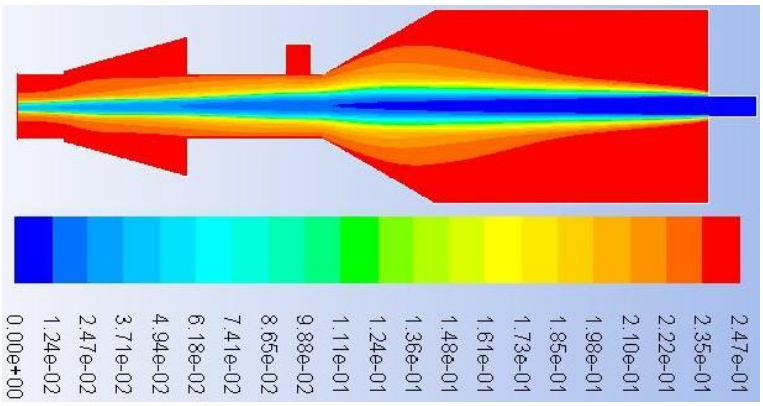

Figure 5.11: Contours of Carbon dioxide

The contours and graphical representation of hydrogen are shown in Figures 5.12 and 5.13, respectively. The hydrogen (H2) mole fraction inside the reactor is 0 to 0.259, while along with the depth of the reactor its composition increases from 0 to 0.016. The increase in the concentration of hydrogen is due to steam methane reaction and water gas shift reaction, as they involved the formation of hydrogen.

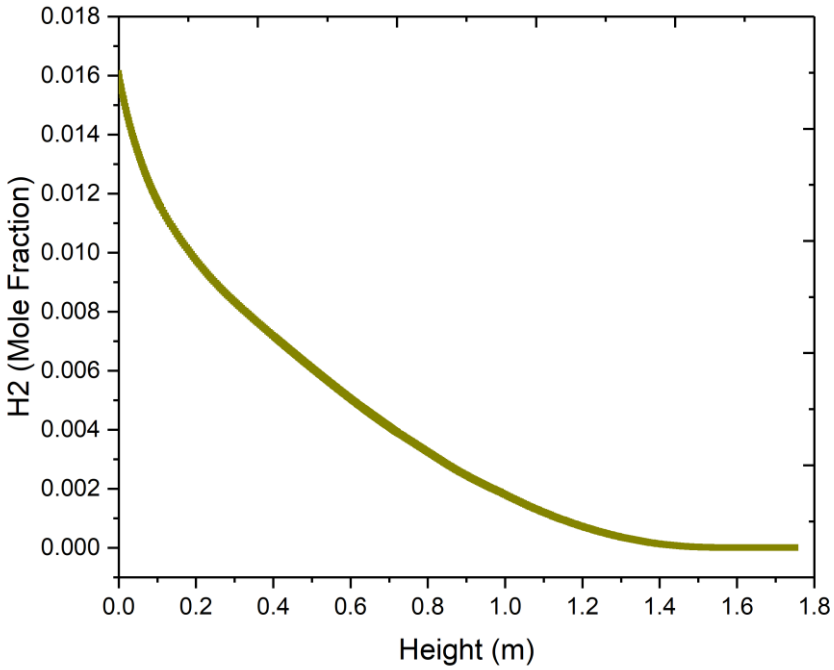

Figure 5.12: Hydrogen profile along with the height of the reactor

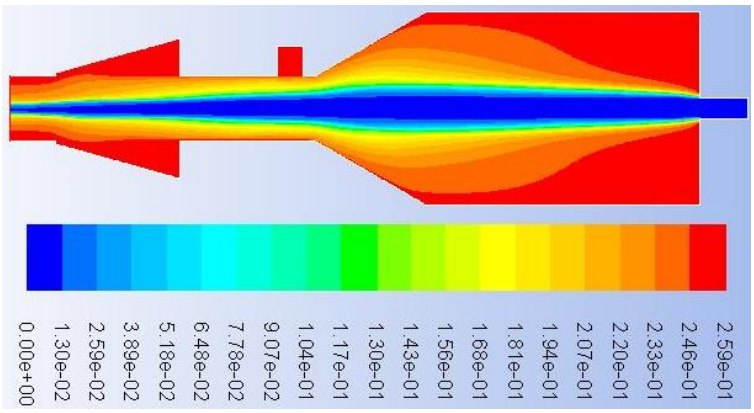

Figure 5.13: Contours of Hydrogen

The mole fraction of methane (CH4) via graphs and contours are shown in Figures 5.14 and 5.15. The mole fraction of methane is from 0 mole percent to 0.0027 mole percent. The behavior of methane concentration shows that it increases as the height of the reactor decreases. The methane gas produces while pyrolysis or tar cracking reaction. Therefore, it rises in the start and becomes almost constant in the latter half of the reactor due to its involvement in steam methane reforming and methane combustion reactions, as shown in Table 1.

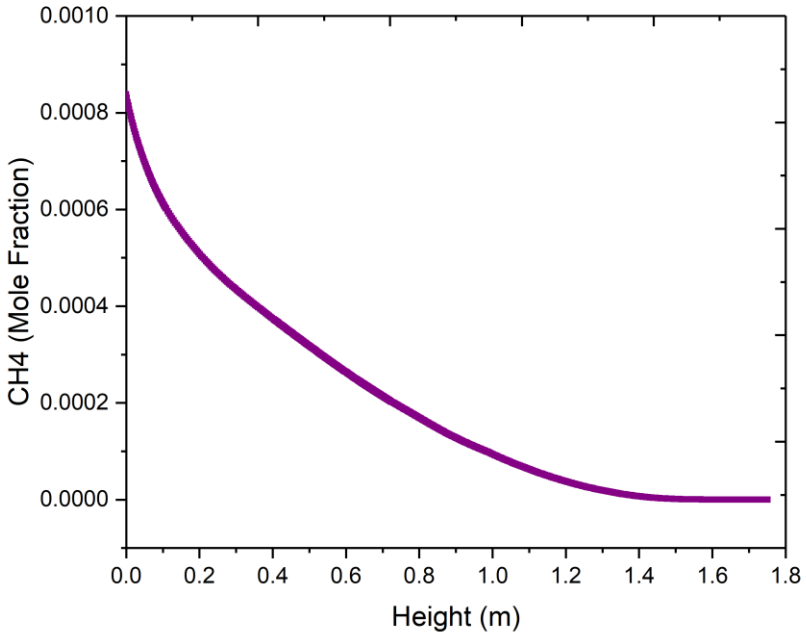

Figure 5.14: Methane profile along with the height of the reactor

In literature, a similar trend was represented for CH_4, as the temperature increases the composition of CH_4 also increases [10].

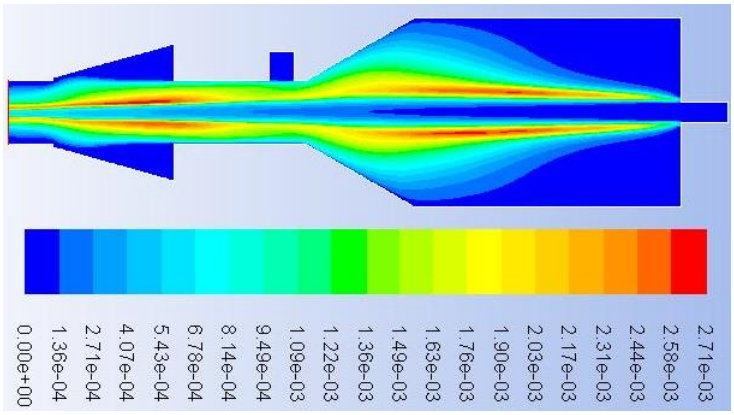

Figure 5.15: Contours of methane

The formation of ethylene (C2H4) occurs when tar cracking takes place and after that its concentration starts decreasing along the length of the reactor as shown in Figures 5.16 and 5.17, respectively.

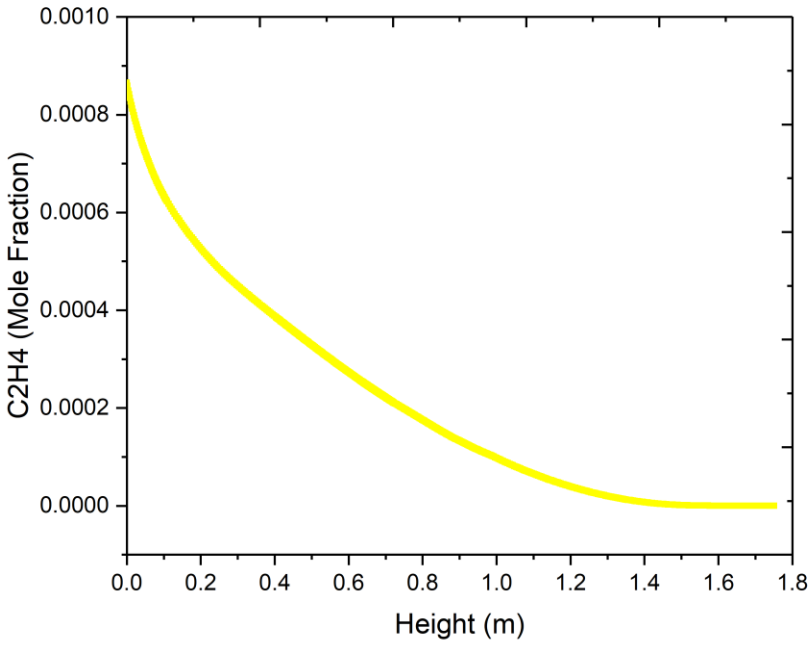

Figure 5.16: Ethylene profile along with the height of the reactor.

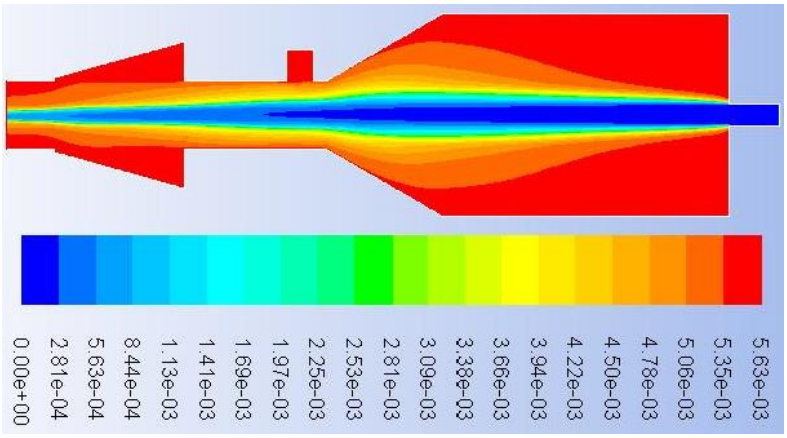

Figure 5.17: Contours of ethylene

The graphical representation and contours of char (unconverted carbon, C) composition is shown in Figures 5.18 and 5.19, respectively. The mole fraction of char (C) is varied from 0 mole percent to 0.007 mole percent inside the reactor. Char composition decreases along the length of reactor as shown in Figure 18.

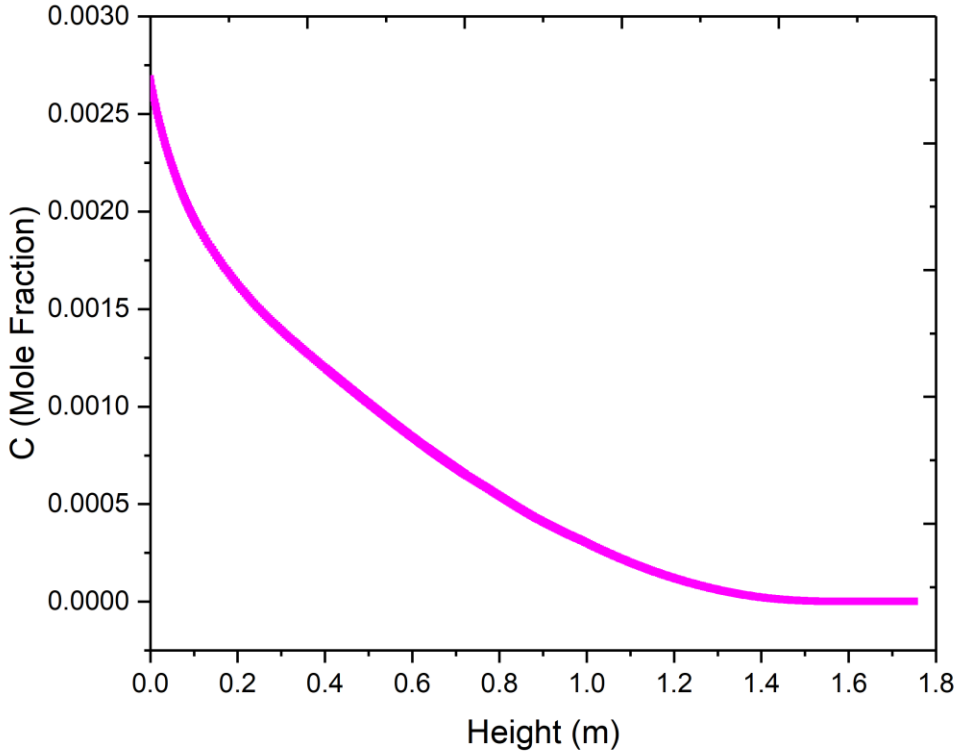

Figure 5.18: Char profile along with the height of the reactor

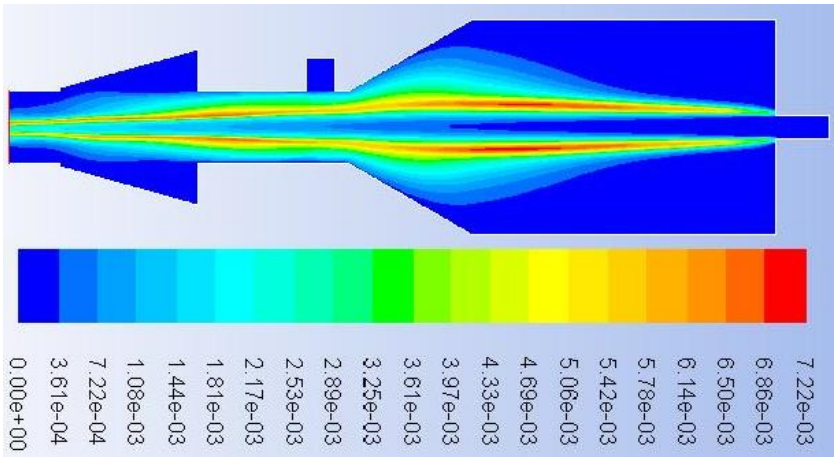

Figure 5.19: Contours of Char

The graphical representation of water and contours formation is shown in Figures 5.20 and 5.21, respectively. The mole fraction of water is 0 to 0.022 mole\%. Water composition decreases along the length of the reactor, as shown in Figure 20.

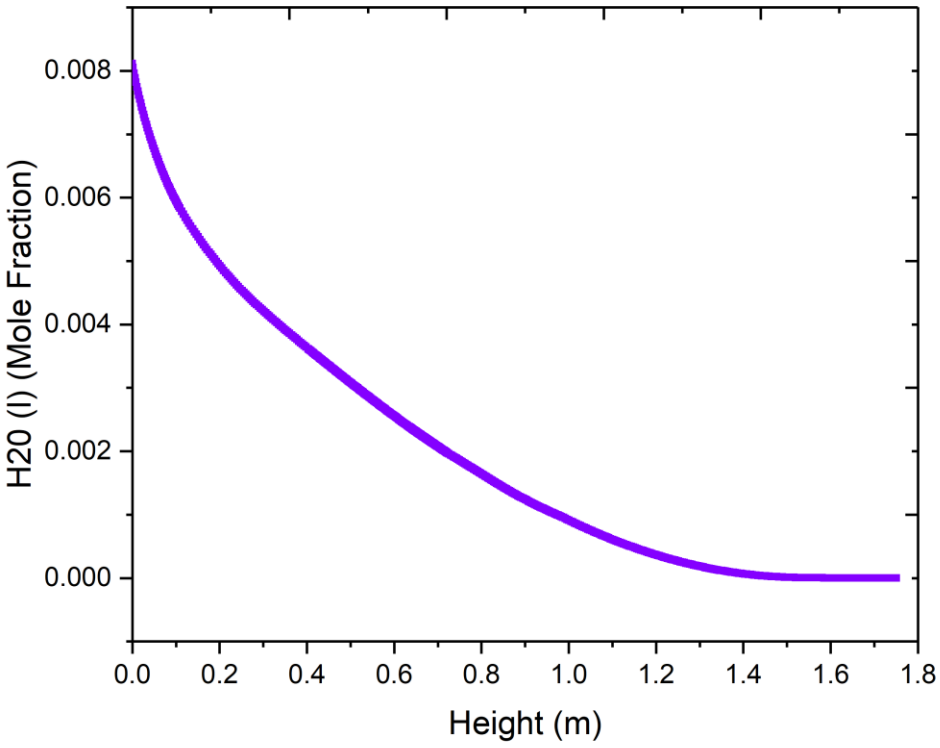

Figure 5.20: Water Profile along with the height of the reactor

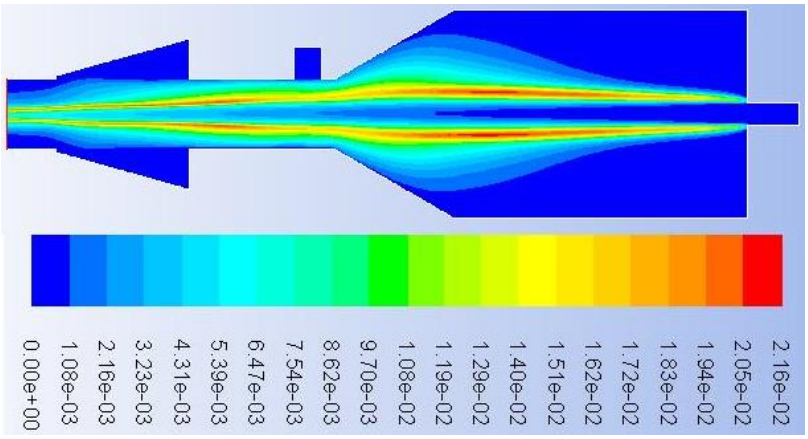

Figure 5.21: Contours of Water

The graphical representation and contours of ammonia are shown in Figures 5.22 and 5.23, respectively. The variation of ammonia (NH3) mole fraction is between 0 to 0.00048 mole

percent inside the reactor. At the same time, its composition decreases along the length of the reactor.

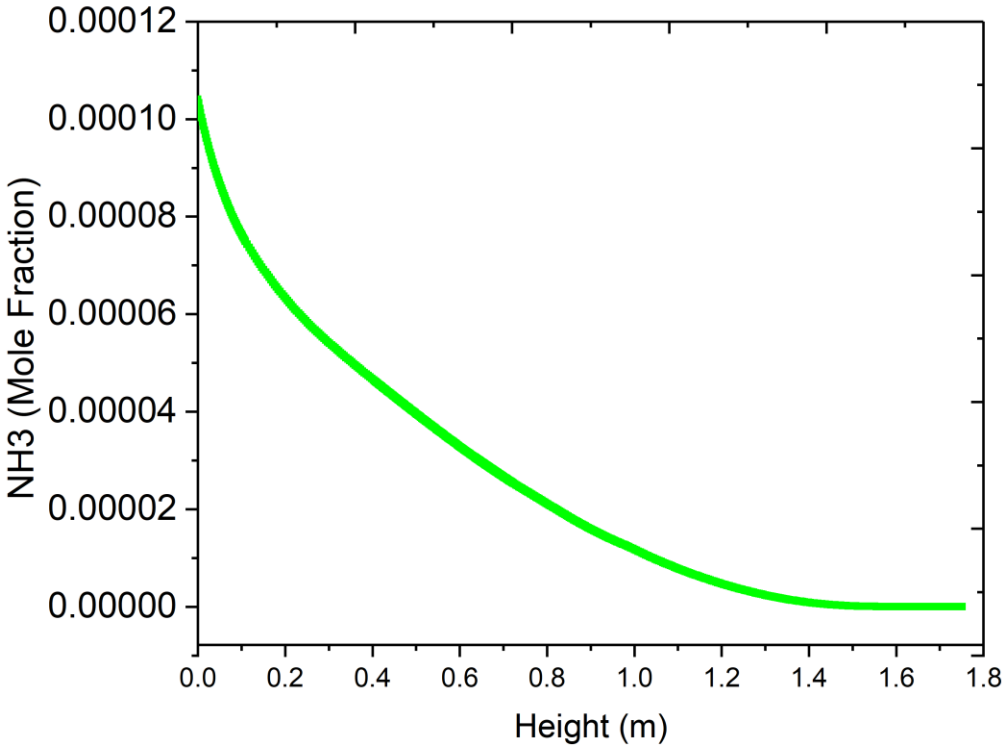

Figure 5.22: Ammonia profile along with the height of the reactor

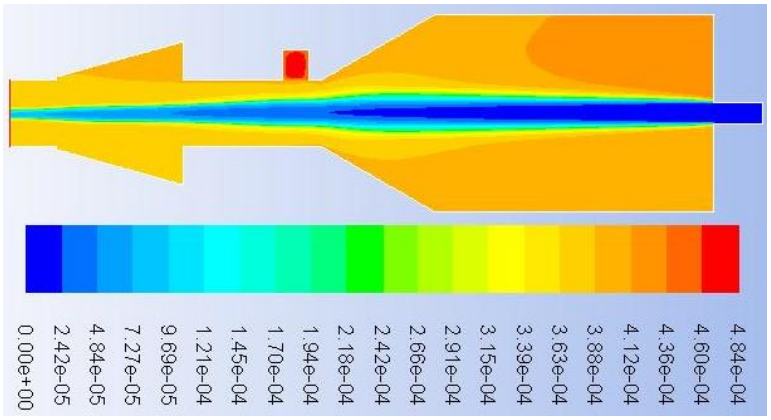

Figure 5.23: Contours of Ammonia

The Graphical profile and contours of hydrogen sulfide in the reactor are shown in Figures 5.24 and 5.25, respectively. The composition of hydrogen sulfide (H2S) inside the reactor is 0 to 9.9e-05 mole\%. Whereas, its composition starts decreasing as the height of the reactor decreases.

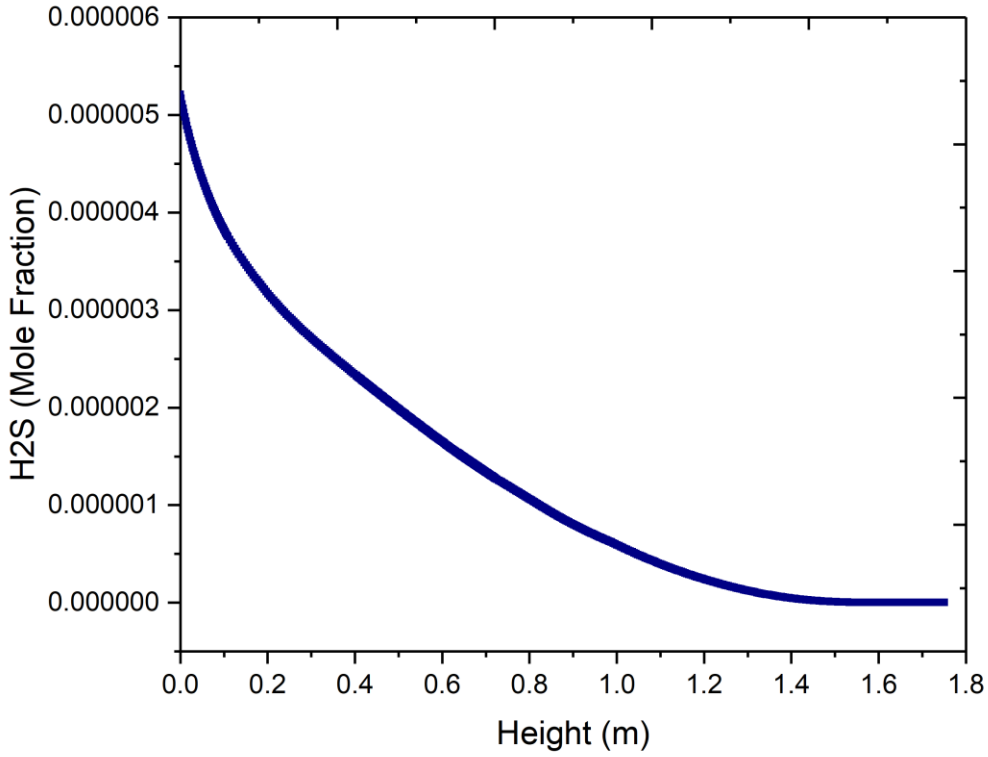

Figure 5.24: Hydrogen sulfide profile along with the height of the reactor

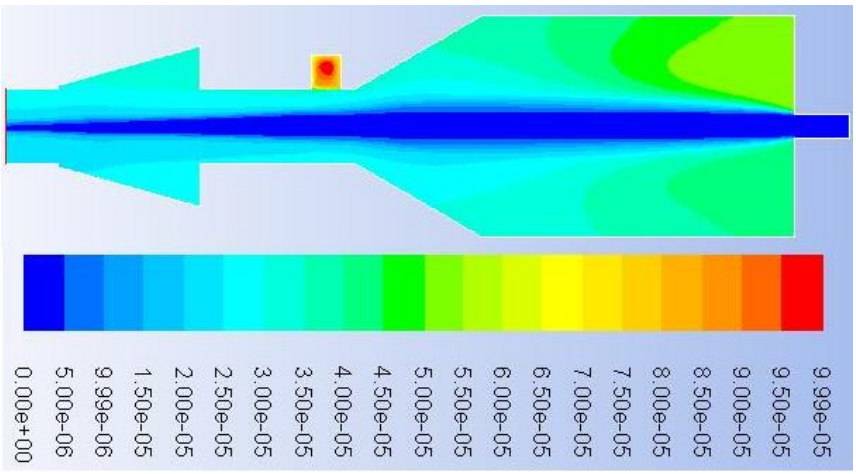

Figure 5.25: Contours of Hydrogen Sulfide

The primary tar profile along the reactor and contours height is shown in Figures 5.26 and 5.27, respectively. The mole fraction of primary tar in the reactor lies between 0 to 0.00203 mole percent. As the height of the gasifier decreases the composition of primary tar increases.

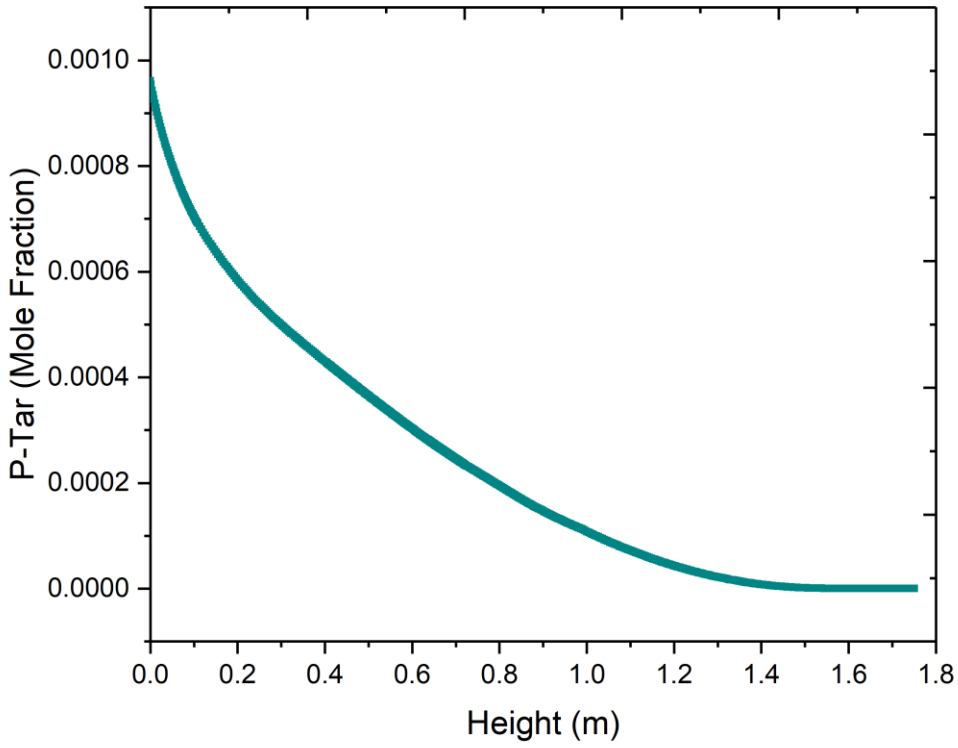

Figure 5.26: Primary tar profile along with the height of the reactor

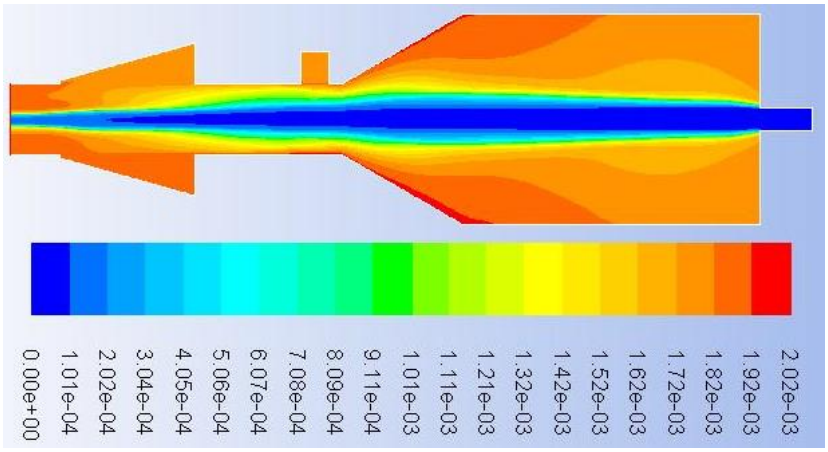

Figure 5.27: Contours of primary tar

The graph of secondary tar and contours of secondary tar are shown in Figures 5.28 and 5.29, respectively. The mole fraction of secondary tar in the reactor lies between 0 to 0.00297 mole%. Secondary tar composition decreases along with the height of the reactor.

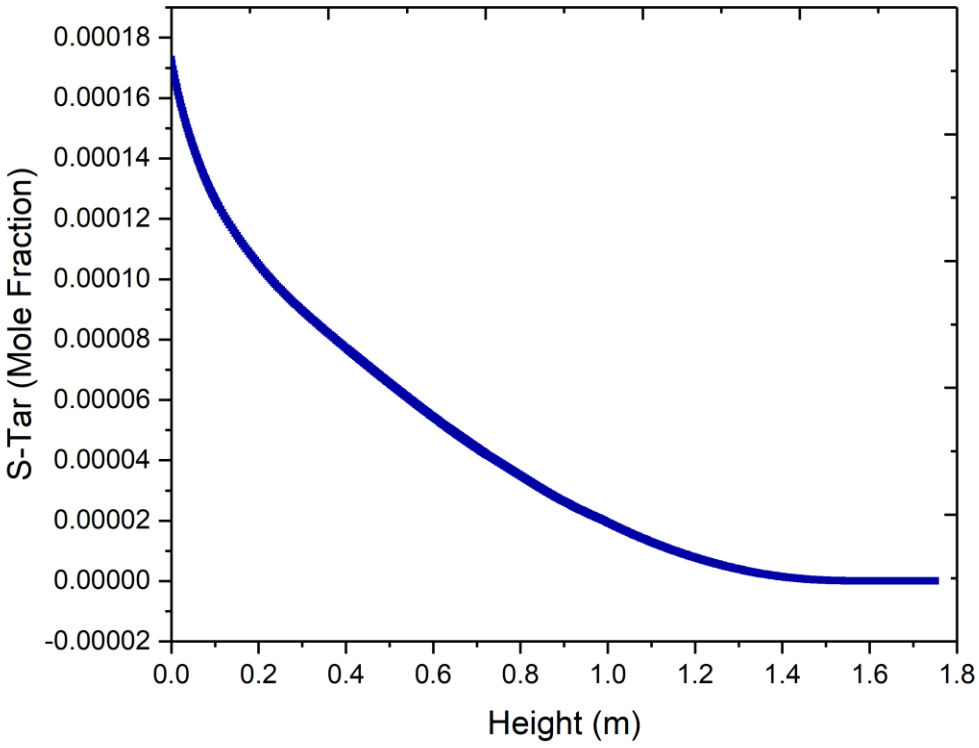

Figure 5.28: S-Tar profile along with the height of the reactor

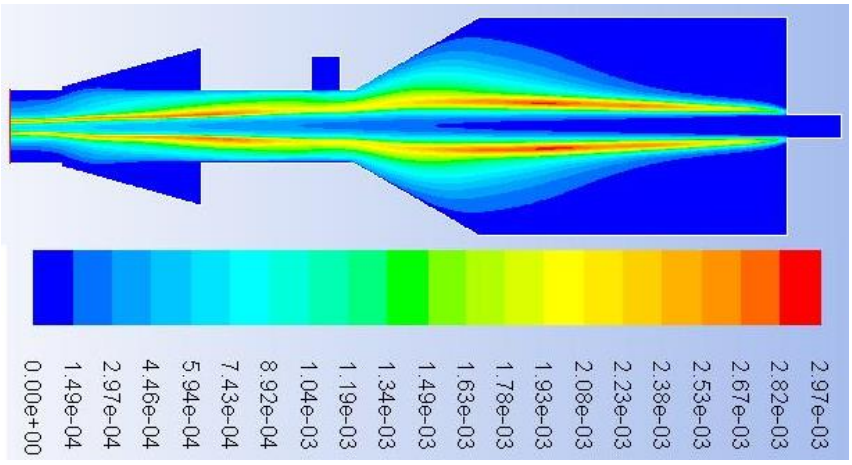

Figure 5.29: Contours of S-Tar

5.3 Exergy Analysis

Figures 5.30 and 5.31 show the graphical and contours representation of mixing exergy. The mixing exergy of components present in the reactor decreases from 2.84E+08 to -

6.54E+07 j/sec. This behavior is due to the high mixing exergy of pure components than the mixing exergy of a mixed form of the components [11]. When the reaction occurs in the gasifier, products readily form these newly produced species intensify gasifier's mixing. This effect produced by products cause irreversibilities and destruct the overall exergy of components in the reactor [7].

Figure 5.30 and 5.32 shows the graphical and contours representation of physical exergy. The physical exergy increases from 0 to 6.37E+15 j/sec. At the inlet of the reactor, the quantity of physical exergy is low, but it increases at the later part of the reactor. The physical exergy decreases as the length of the reactor increases due to irreversibility caused by the temperature drop along the length of the reactor. In literature it is stated that the physical exergy of the reactor is dropped where the temperature of the reactor is decreased [12].

The contours and graphical representation of chemical exergy as shown in Figure 5.30 and 5.33, respectively. The chemical exergy increases from -1.267E+16 to 3.036E+14 j/sec. The chemical reaction occurs in a gasifier and syngas and other components are produced during the chemical reaction. These components increase the chemical exergy [13].

The contours and graphs of total exergy are as shown in Figure 5.30 and 5.34, respectively. The total exergy is in the range of -6.46E+15 to 7.38E+14 j/sec. The total exergy is the combined effect of chemical, mixing, and physical exergies. The amount of total exergy is increased as the reaction takes place due to the summation of physical, mixing, and chemical exergy. This increasing effect represents the higher potential of syngas produced during the reaction.

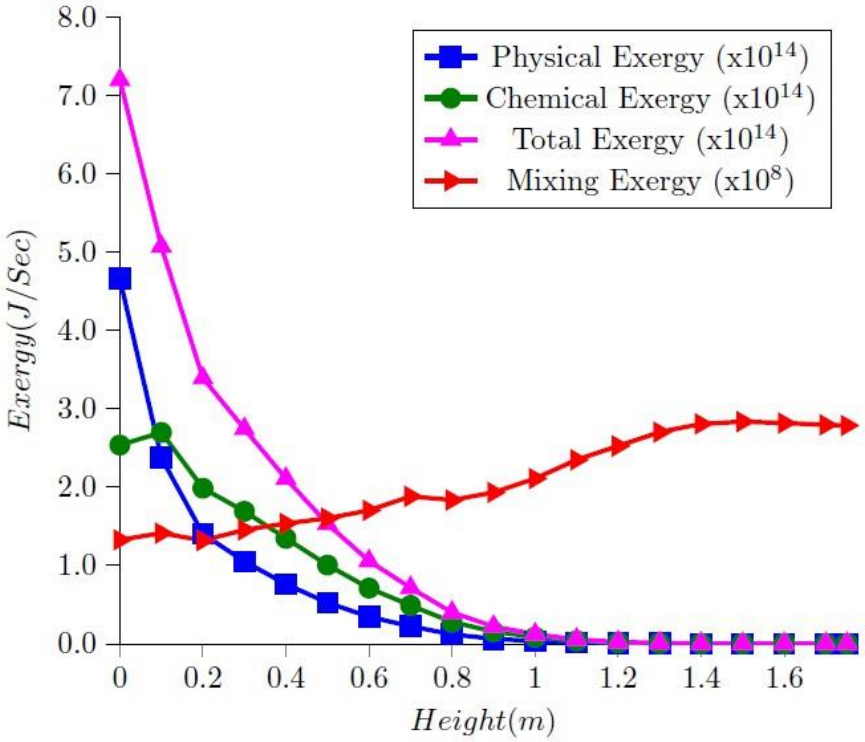

Figure 5.30: Physical, Chemical, Mixing and Total Exergy profile along with the height of the reactor

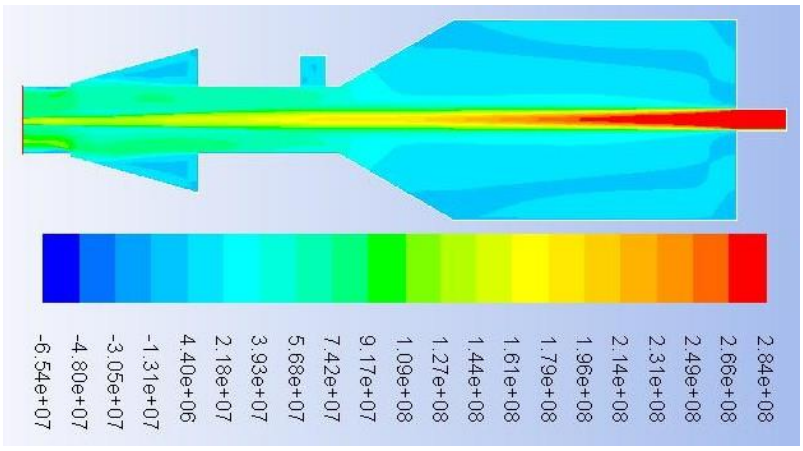

Figure 5.31: Contours of mixing exergy

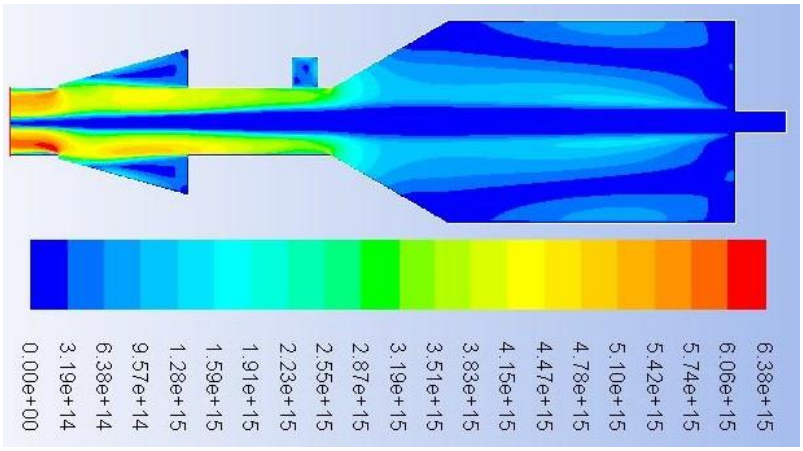

Figure 5.32: Contours of physical exergy

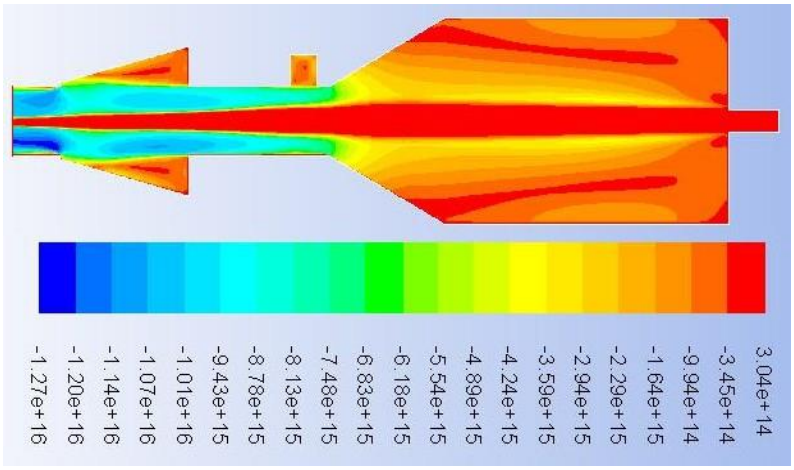

Figure 5.33: Contours of Chemical Exergy

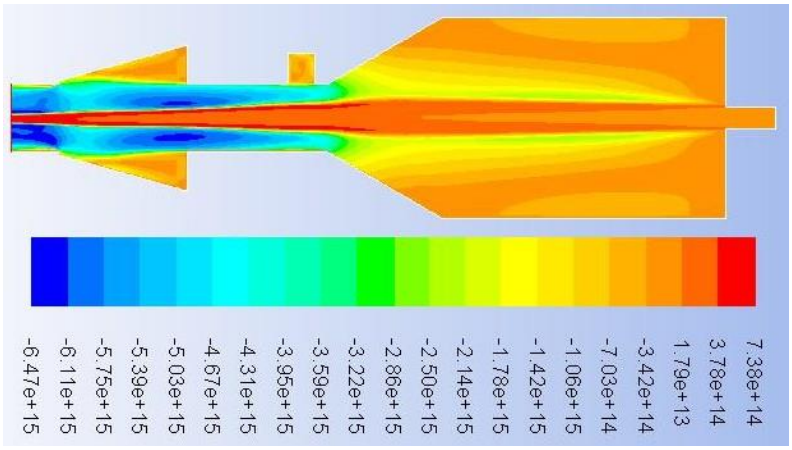

Figure 5.34: Contours of Total Exergy

Summary

The high temperature is required for production of combustible gases. The syngas ratio of 1.55:1 is observed. As the temperature of gasification increases the production of CO also increases, which results in increase in syngas ratio. The total exergy of biomass gasifier shows that it has potential of 7.38E+14 j/sec to perform work.

References:

[1] M. S. and Xiang Luo, Tao Wu, Kaiqi Shi and Y. Rao, "Biomass Gasification: An Overview of Technological Barriers and Socio-Environmental Impact," in *Gasification for Low-grade Feedstock*, Yongseung Yun, Ed. IntechOpen, 2018, p. 290.

[2] M. A. Chawdhury and K. Mahkamov, "Development of a Small Downdraft Biomass Gasifier for Developing Countries," *J. Sci. Res.*, vol. 3, no. 1, p. 51, 2010.

[3] L. S. Ã, Y. Gao, and J. Xiao, "Simulation of hydrogen production from biomass gasification in interconnected fluidized beds," vol. 32, pp. 120–127, 2008.

[4] Z. Li, H. Xu, W. Yang, A. Zhou, and M. Xu, "CFD simulation of a fluidized bed reactor for biomass chemical looping gasification with continuous feedstock," *Energy Convers. Manag.*, vol. 201, no. September, p. 112143, 2019.

[5] U. Lee, E. Balu, and J. N. Chung, "An experimental evaluation of an integrated biomass gasification and power generation system for distributed power applications," *Appl. Energy*, vol. 101, pp. 699–708, 2013.

[6] R. Karamarkovic and V. Karamarkovic, "Energy and exergy analysis of biomass gasification at different temperatures," *Energy*, vol. 35, no. 2, pp. 537–549, 2010.

[7] Z. ur Rahman, I. Ahmad, M. Kano, and J. Mustafa, "Model development and exergy analysis of a microreactor for the steam methane reforming process in a CFD environment," *Entropy*, vol. 21, no. 4, pp. 1–19, 2019.

[8] J. Han *et al.*, "Modeling downdraft biomass gasification process by restricting chemical reaction equilibrium with Aspen Plus," *Energy Convers. Manag.*, vol. 153,

no. August, pp. 641–648, 2017.

[9] S. Rupesh, C. Muraleedharan, and P. Arun, “ASPEN plus modelling of air–steam gasification of biomass with sorbent enabled CO2 capture,” *Resour. Technol.*, vol. 2, no. 2, pp. 94–103, 2016.

[10] T. Damartzis, S. Michailos, and A. Zabaniotou, “Energetic assessment of a combined heat and power integrated biomass gasification-internal combustion engine system by using Aspen Plus®,” *Fuel Process. Technol.*, vol. 95, pp. 37–44, 2012.

[11] N. Sato, *Chemical energy and exergy: An introduction to chemical thermodynamics for engineers*, 1st Editio. Elsevier Science, 2004.

[12] A. U. Akram, I. Ahmad, A. Chughtai, and M. Kano, “Exergy analysis and optimisation of naphtha reforming process with uncertainty,” *Int. J. Exergy*, vol. 26, no. 3, pp. 247–262, 2018.

[13] J. Mustafa, I. Ahmad, M. Ahsan, and M. Kano, “Computational fluid dynamics based model development and exergy analysis of naphtha reforming reactors,” *Int. J. Exergy*, vol. 24, no. 2–4, pp. 344–363, 2017.

Conclusions and Future Recommendations

In this work, the downdraft biomass gasifier's exergy analysis was performed using the CFD model. To incorporate the reaction mechanism a species transport model was used. For higher production of syngas, optimized operating conditions were used. Then, the evaluation of exergy of the biomass gasifier was occurred by means of a CFF. The exergy analysis evaluated all three types of exergy analysis, chemical exergy, physical exergy, and mixing exergy, in the downdraft biomass gasifier. As the temperature of the gasifier increases due to exothermic reactions, the physical exergy increases. The high rate of product formation like syngas, carbon dioxide, etc. increases chemical exergy. On the other hand, the gasifier's mixing effect in the gasifier caused the irreversibility, which decreases the mixing exergy.

In future work, exergy analysis can be performed by interfacing MATLAB®-Aspen PLUS® model. The sensitivity analysis of the model can be done to get better synthesis gas composition. The sensitivity analysis helps in evaluating the efficiency of a model by changing individual parameters of the model.

Appendix A

Exergy Codes:

Physical Exergy:

a1 = ((1.45*10^7)*(ln (Total pressure/101325))*(|v|/total temperature))

a = mole-CO*a1

b = mole-CO2*a1

c1= mole-h2*a1

d = mole-Ch4*a1

e = mole-C2h4*a1

f = mole-C*a1

g = mole-ash*a1

h = mole-h2o $_{(Steam)}$*a1

i = mole-h2o $_{(liq)}$*a1

j = mole-h2s*a1

k= mole-n2*a1

l = mole-nh3*a1

m = mole-o2*a1

n = mole-Ptar*a1

o = mole-Star*a1

p = mole-wood*a1

th = (1.45*10^7*(|V|/total temperature)*(total temperature – 273 – 273*ln (total temperature/ 273))

Cp_co = (molef-co * 8.314 * ((3.71 * (total-temperature - 273)) - (((0.899 * 10 ^ (- 3)) / 2) * ((total-temperature ^ 2) - (273 ^ 2))) + (((1.14 * 10 ^ (- 6)) / 3) * ((total-temperature ^ 3) - (273 ^ 3))) - (((0.348 * 10 ^ (- 9)) / 4) * ((total-temperature ^ 4) - (273 ^ 4))) + (((0.0228 * 10 ^ (- 12)) / 5) * ((total-temperature ^ 5) - (273 ^ 5))))))

Cp_co2 = ((molef-co2 * 8.314 * ((2.401 * (total-temperature - 273)) + (((4.853 * 10 ^ (- 3)) / 2) * ((total-temperature ^ 2) - (273 ^ 2))) - (((2.039 * 10 ^ (- 6)) / 3) * ((total-

temperature ^ 3) - (273 ^ 3))) + (((0.343 * 10 ^ (- 9)) / 4) * ((total-temperature ^ 4) - (273 ^ 4))))))

Cp_h_2 = (molef-h2 * 8.314 * ((3.057 * (total-temperature - 273)) + (((1.487 * 10 ^ (- 3)) / 2) * ((total-temperature ^ 2) - (273 ^ 2))) - (((1.793 * 10 ^ (- 6)) / 3) * ((total-temperature ^ 3) - (273 ^ 3))) + (((0.947 * 10 ^ (- 9)) / 4) * ((total-temperature ^ 4) - (273 ^ 4))) - (((0.1726 * 10 ^ (- 12)) / 5) * ((total-temperature ^ 5) - (273 ^ 5)))))

Cp_CH_4 = (molef-ch4 * 8.314 * ((3.826 * (total-temperature - 273)) - (((2.211 * 10 ^ (- 3)) / 2) * ((total-temperature ^ 2) - (273 ^ 2))) + (((7.580 * 10 ^ (- 6)) / 3) * ((total-temperature ^ 3) - (273 ^ 3))) - (((3.889 * 10 ^ (- 9)) / 4) * ((total-temperature ^ 4) - (273 ^ 4))) + (((0.6633 * 10 ^ (- 12)) / 5) * ((total-temperature ^ 5) - (273 ^ 5)))))

Cp_C_2H_4 = (molef-c2h4 * 8.314 * ((1.426 * (total-temperature - 273)) + (((6.234 * 10 ^ (- 3)) / 2) * ((total-temperature ^ 2) - (273 ^ 2))) - (((7.562 * 10 ^ (- 6)) / 3) * ((total-temperature ^ 3) - (273 ^ 3))) + (((2.811 * 10 ^ (- 9)) / 4) * ((total-temperature ^ 4) - (273 ^ 4))) - (((0.3939 * 10 ^ (- 12)) / 5) * ((total-temperature ^ 5) - (273 ^ 5)))))

Cp_Char = (molef-c * 0.084 * ((2.673 * (total-temperature - 273)) + (((2.617 * 10 ^ (- 3)) / 2) * ((total-temperature ^ 2) - (273 ^ 2))) + (116900 / (total-temperature - 273))))

Cp_ASH = (molef-ash * (2.42 * 10 ^ (- 4)) * (795 * (total-temperature - 273)))")

Cp_h2ol = ((1.34 * 10 ^ (- 8)) * molef-h2o<l> * ((276.37 * (total-temperature - 273)) - (((2090.1) / 2) * ((total-temperature ^ 2) - (273 ^ 2))) + (((8.125) / 3) * ((total-temperature ^ 3) - (273 ^ 3))) - (((0.014116) / 4) * ((total-temperature ^ 4) - (273 ^ 4))) + (((9.37 * 10 ^ (- 6)) / 5) * ((total-temperature ^ 5) - (273 ^ 5)))))

Cp_h2o = (molef-h2o * 8.314 * ((4.070 * (total-temperature - 273)) - (((0.616 * 10 ^ (- 3)) / 2) * ((total-temperature ^ 2) - (273 ^ 2))) + (((1.28 * 10 ^ (- 6)) / 3) * ((total-temperature ^ 3) - (273 ^ 3))) - (((0.508 * 10 ^ (- 9)) / 4) * ((total-temperature ^ 4) - (273 ^ 4))) + (((0.0769 * 10 ^ (- 12)) / 5) * ((total-temperature ^ 5) - (273 ^ 5)))))

Cp_H_2S = (0.0297 * molef-h2s * ((7.20 * (total-temperature - 273)) + (((0.0036) / 2) * ((total-temperature ^ 2) - (273 ^ 2)))))

Cp_N_2 = (molef-n2 * 8.314 * ((3.675 * (total-temperature - 273)) - (((0.671 * 10 ^ (- 3)) / 2) * ((total-temperature ^ 2) - (273 ^ 2))) + (((0.717 * 10 ^ (- 6)) / 3) * ((total-temperature ^ 3) - (273 ^ 2))) - (((0.108 * 10 ^ (- 9)) / 4) * ((total-temperature ^ 4) - (273 ^ 4))) - (((0.0215 * 10 ^ (- 12)) / 5) * ((total-temperature ^ 5) - (273 ^ 5)))))

Cp_NH_3 = (molef-nh3 * 8.314 * ((3.591 * (total-temperature - 273)) + (((0.274 * 10 ^ (- 3)) / 2) * ((total-temperature ^ 2) - (273 ^ 2))) + (((2.576 * 10 ^ (- 6)) / 3) * ((total-temperature ^ 3) - (273 ^ 3))) - (((1.437 * 10 ^ (- 9)) / 4) * ((total-temperature ^ 4) - (273 ^ 4))) + (((0.2601 * 10 ^ (- 12)) / 5) * ((total-temperature ^ 5) - (273 ^ 5)))))

Cp_O_2 = (molef-o2 * 8.314 * ((3.626 * (total-temperature - 273)) - (((1.043 * 10 ^ (- 3)) / 2) * ((total-temperature ^ 2) - (273 ^ 2))) + (((2.178 * 10 ^ (- 6)) / 3) * ((total-temperature

^ 3) - (273 ^ 3))) - (((1.16 * 10 ^ (- 9)) / 4) * ((total-temperature ^ 4) - (273 ^ 4))) + (((0.2053 * 10 ^ (- 12)) / 5) * ((total-temperature ^ 5) - (273 ^ 5)))))

Cp_P_Tar = (molef-c6.407h11.454o3.482 * (2.42 * 10 ^ (- 4)) * ((1663 * (total-temperature - 273))))

Cp_ S_Tar = (3.1 * 10 ^ (- 9) * molef-c6h6 * ((129440 * (total-temperature - 273)) - (((169.5) / 2) * ((total-temperature ^ 2) - (273 ^ 2))) + (((0.64781) / 3) * ((total-temperature ^ 3) - (273 ^ 3)))))

Cp_Wood = (molef-wood_vol * (2.42 * 10 ^ (- 4)) * (1500 * (total-temperature - 273)))

Physical Exergy = (a + b + c1 + d + e + f + g + h + i + j + k + l + m + n + o + p) + (th * (cp_co + cp_co2 + cp_h2 + cp_ch4 + cp_c2h4 + cp_char + cp_ash + cp_h20l + cp_h2o + cp_h2s + cp_n2 + cp_nh3 + cp_o2 + cp_p_tar + cp_s_tar + cp_wood))

Chemical Exergy:

Ch = (1.45 * 10 ^ 7 * (|V| / total-temperature))

ch_h2ol = ((- 237.178 * (ch * molef-h2o<l>)) + (i + (th * cp_h20l)))

ch_co = ((- 137.277 * (ch * molef-co)) + (a + (th * cp_co)))

ch_co2 = ((- 394.383 * (ch * molef-co2)) + (b + (th * cp_co2)))

ch_ch4 = ((- 50.836 * (ch * molef-ch4)) + (d + (th * cp_ch4)))

ch_h2 = (c1 + (th * cp_h2))

ch_h2o = ((- 228.589 * (ch * molef-h2o)) + (h + (th * cp_h2o)))

ch_nh3 = ((- 16.485 * (ch * molef-nh3<l>)) + (l + (th * cp_nh3)))

ch_h2s = ((- 33.054 * (ch * molef-h2s)) + (j + (th * cp_h2s)))

ch_o2 = (m + (th * cp_o2))

ch_n2 = (k + (th * cp_n2))

ch-c2h4 = ((61.42 * (ch * molef-c2h4)) + (e + (th * cp_c2h4)))

ch_char = ((669.603 * (ch * molef-c)) + (f + (th * cp_char)))

ch_s_tar = ((129.66216 * (ch * molef-c6h6)) + (o + (th * cp_s_tar)))

ch_p_tar = ((2.602 * (ch * molef-c6.407h11.454o3.482)) + (n + (th * cp_p_tar)))

ch_ash = (g + (th * cp_ash))

ch_wood = ((- 254.8 * (ch * molef-wood_vol)) + (p + (th * cp_wood)))

rxn_1 = (ch_wood - ch_h2ol - ch_char - ch_ash - (0.268 * ch_co) - (0.295 * ch_co2) - (0.094 * ch_ch4) - (0.5 * ch_h2) - (0.255 * ch_h2o) - (0.004 * ch_nh3) - (0.0002 * ch_h2s) - (0.2 * ch_p_tar))

rxn_2 = (ch_p_tar - (0.261 * ch_s_tar) - (2.6 * ch_co) - (0.441 * ch_co2) - (0.983 * ch_ch4) - (2.161 * ch_h2) - (0.408 * ch-c2h4))

rxn_3 = ((2 * ch_char) + ch_o2 - (2 * ch_co))

rxn_4 = (ch_char + ch_o2 - ch_co2)

rxn_5 = (ch_char + ch_h2o - ch_co - ch_h2)

rxn_6 = (ch_char + ch_co2 - (2 * ch_co))

rxn_7 = (ch_p_tar + (4.326 * ch_o2) - (5.727 * ch_h2o) - (6.407 * ch_co))

rxn_8 = (ch_s_tar + (4.5 * ch_o2) - (3 * ch_h2o) - (6 * ch_co))

rxn_9 = (ch_h2 + (0.5 * ch_o2) - ch_h2o)

rxn_10 = (ch_co + (0.5 * ch_o2) - ch_co2)

rxn_11 = (ch_co + ch_h2o - ch_h2 - ch_co2)

rxn_12 = (ch_ch4 + (1.5 * ch_o2) - ch_co - (2 * ch_h2o))

rxn_13 = (ch_ch4 + ch_h2o - ch_co - (3 * ch_h2o))

Chemical Exergy: (rxn_1 + rxn_2 + rxn_3 + rxn_4 + rxn_5 + rxn_6 + rxn_7 + rxn_8 + rxn_9 + rxn_10 + rxn_11 + rxn_12 + rxn_13)

Mixing Exergy:

Mixing Exergy: (a + b + c1 + d + e + f + g + h + i + j + k + l + m + n + o + p)

Total Exergy:

Total Exergy: (chemical_exergy + mixing_exergy + physical-exergy)

Appendix B

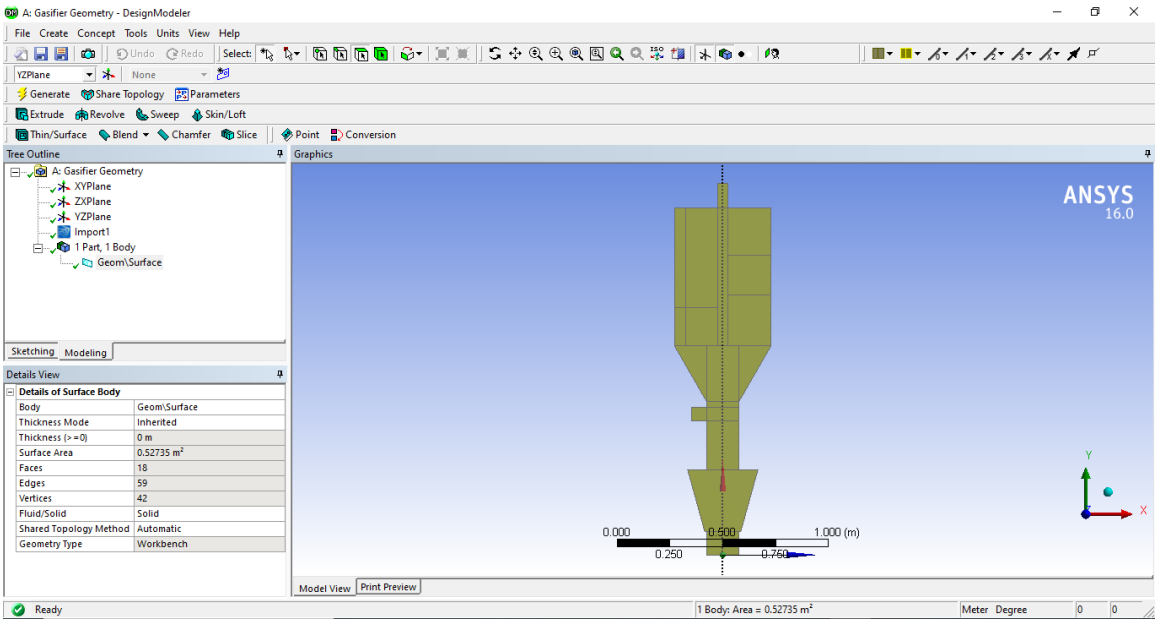

Figure 4.1: Geometry of Lab scale Biomass Gasifier in design modeler

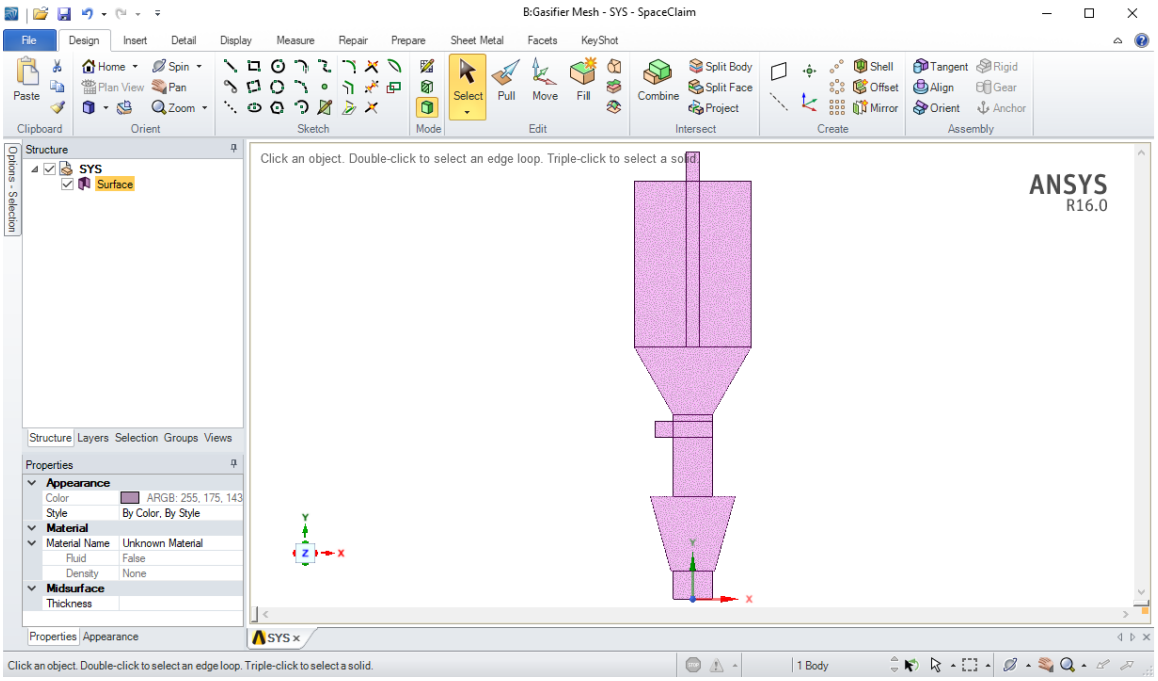

Figure4.2: Face development of biomass gasifier using space claim

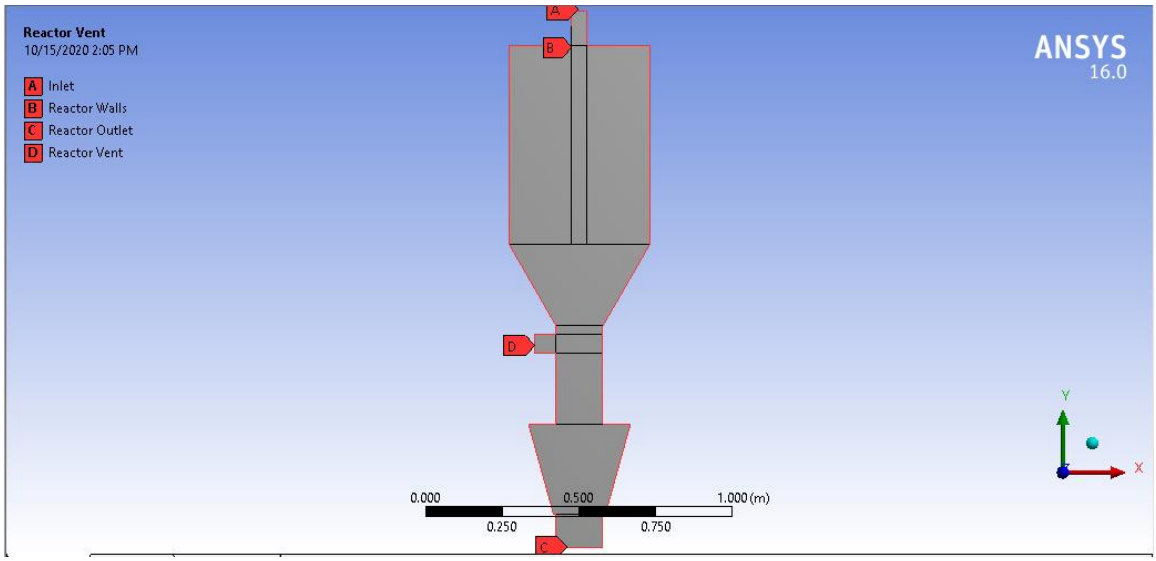

Figure 4.3: Named selection for boundaries

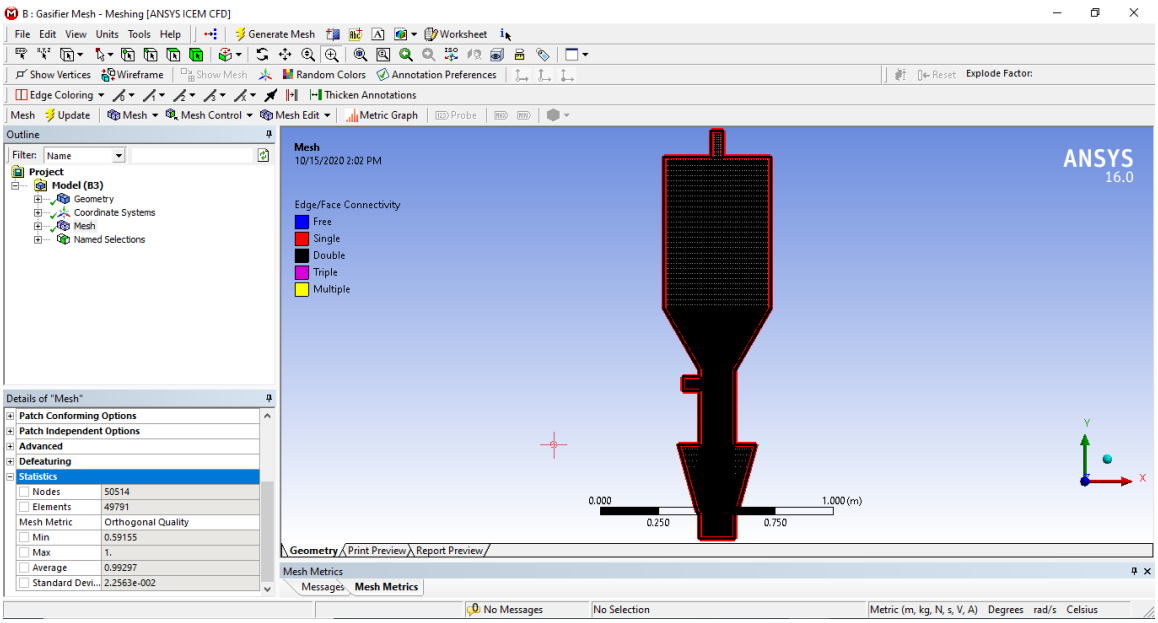

Figure 4.4: Meshing of biomass gasifier using ANSYS Mesh

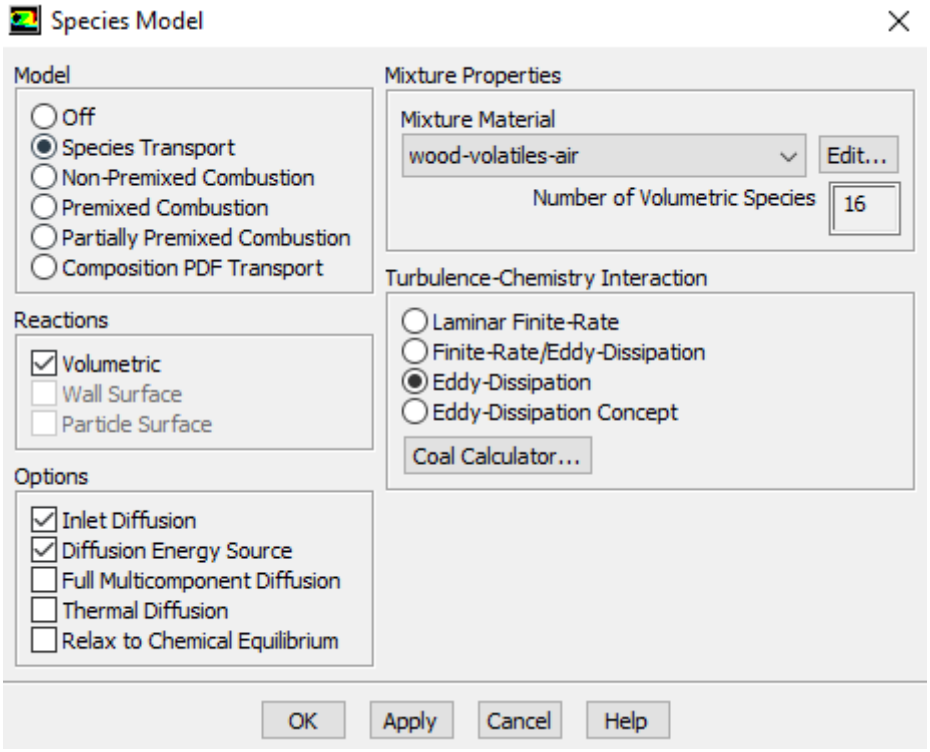

Figure 4.5: Species Transport Model

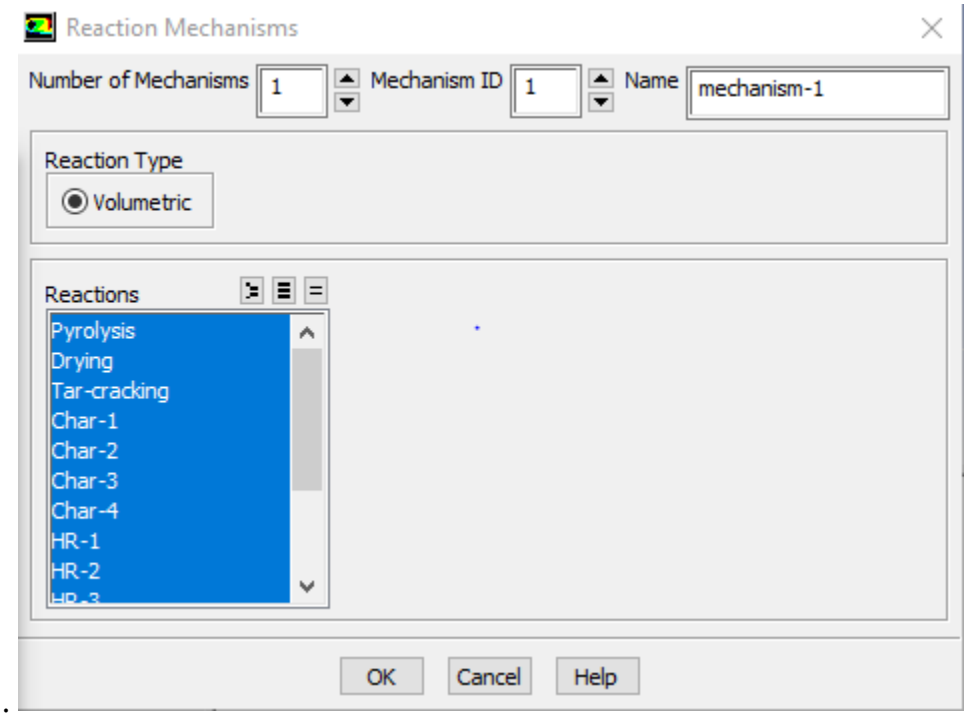

Figure 4.6: Imported Reaction Mechanism

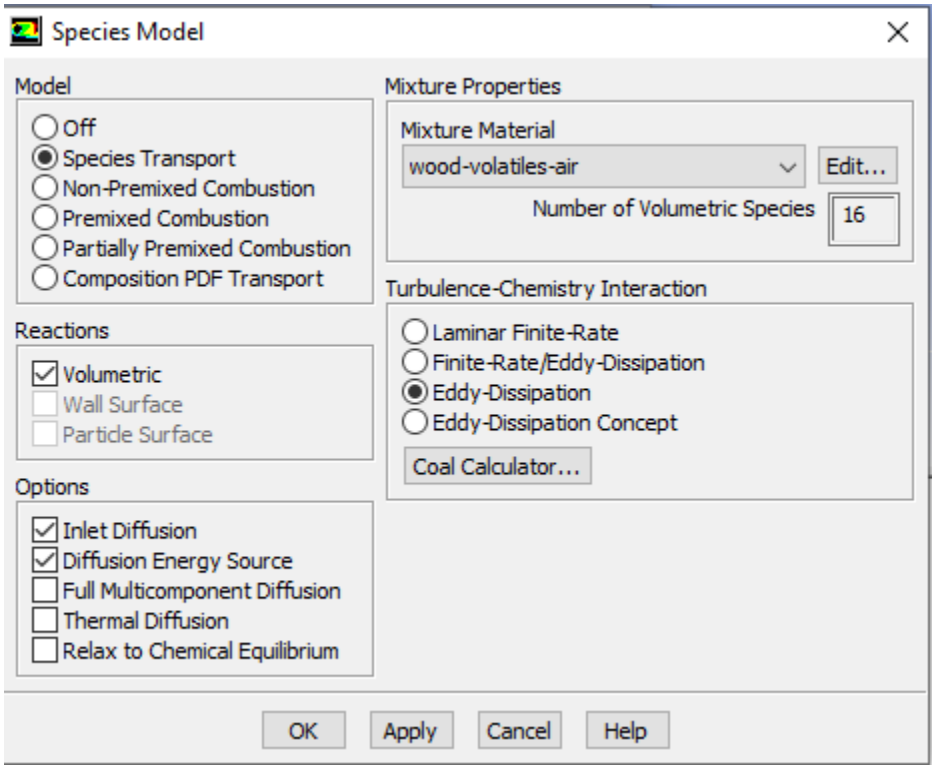

Figure 4.7: Turbulence-Chemistry Interaction

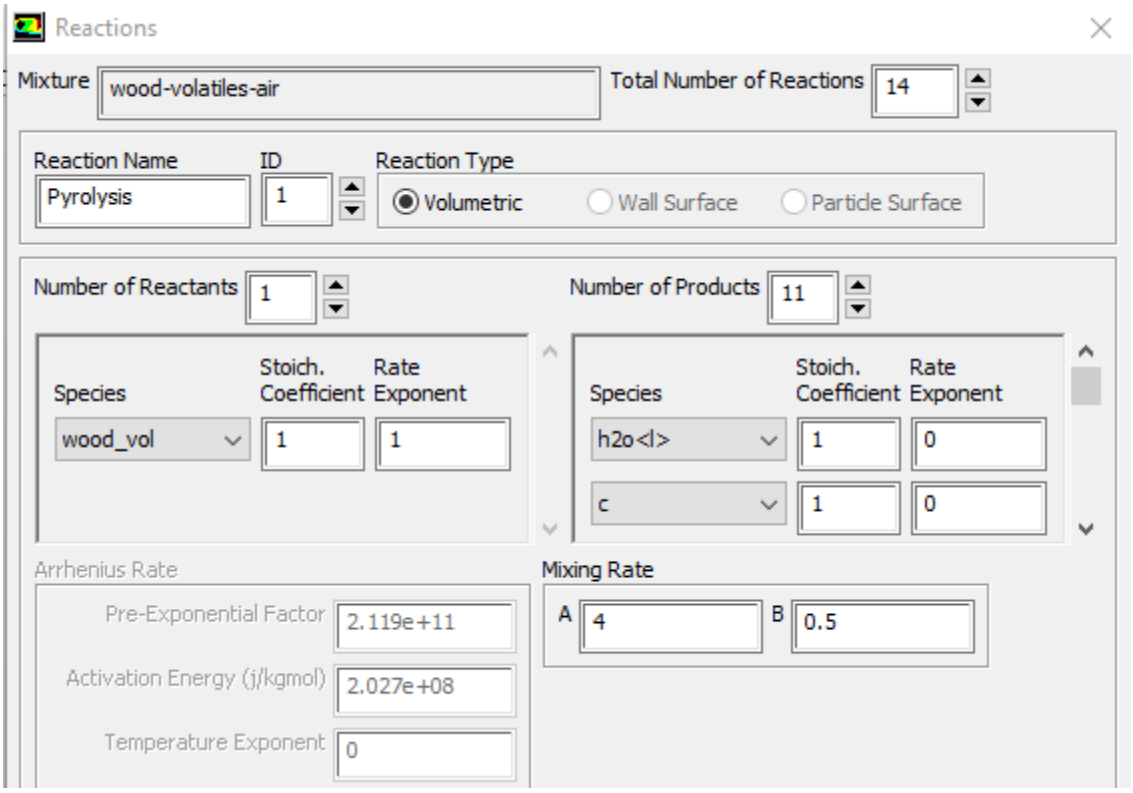

Figure 4.8: Parameter for reaction schema

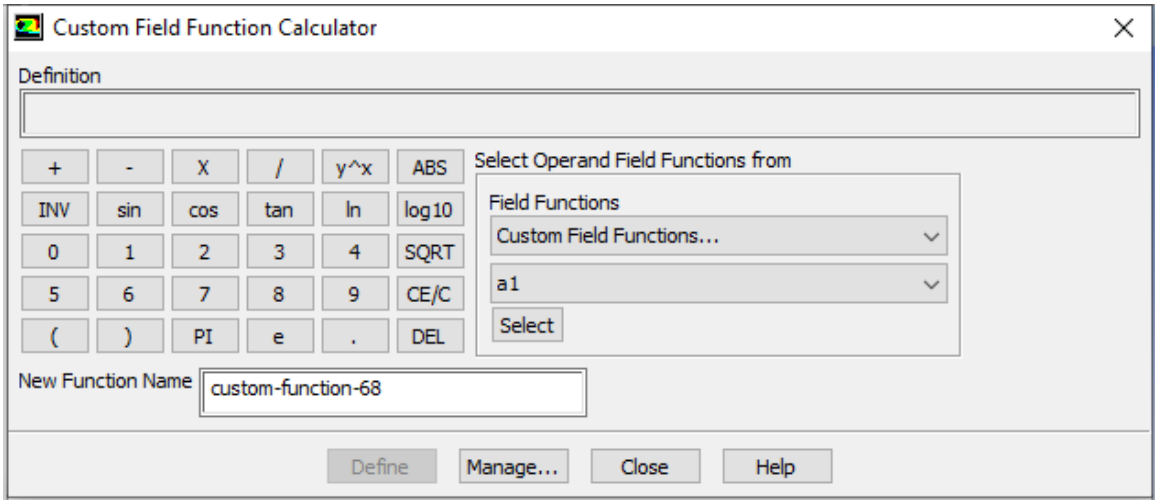

Figure 4.9: CFF Calculator

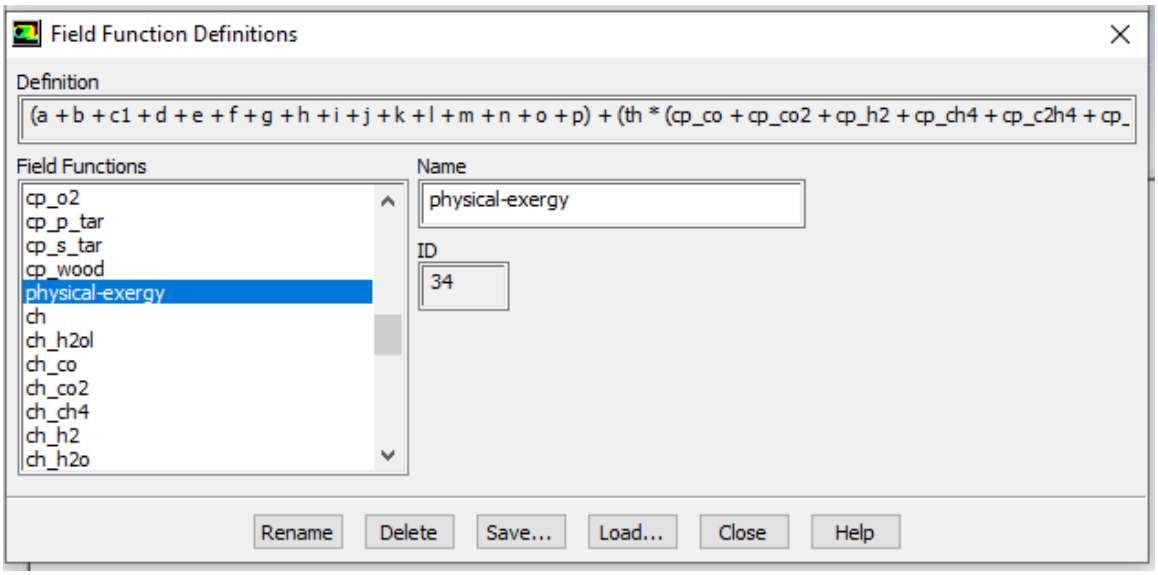

Figure 4.10: Field Function Definition

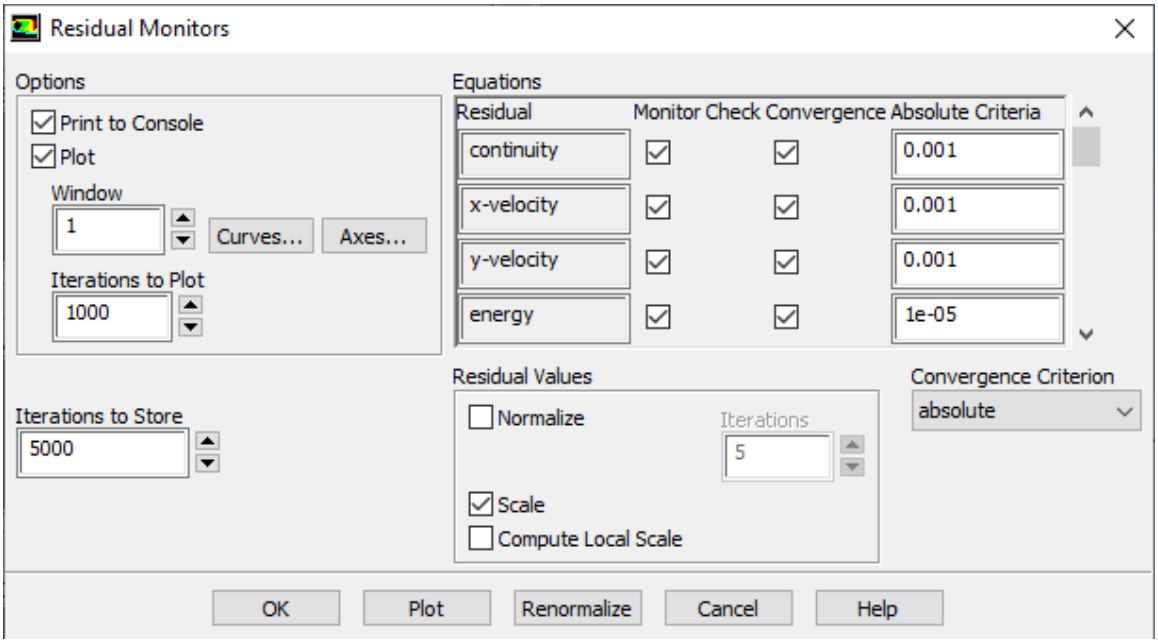

Figure 4.11: Residual Monitors

Appendix C

CFD Based Design and Exergy Analysis of Downdraft Biomass Gasifier

Ahsan Ayub[a], Iftikhar Ahmad[b], Muhammad Hassan*[a], Mustafa Anwar[a]

[a]US Pak Center for Advanced Studies in Energy, National University of Sciences and Technology (NUST), H-12 Islamabad 44000, Pakistan

[b]School of Chemical and Materials Engineering, National University of Sciences and Technology (NUST), H-12 Islamabad 44000, Pakistan

Email address: hassan@uspcase.nust.edu.pk (Muhammad Hassan*)

Current Status: submitted to "International Journal of Computational Fluid Dynamics"

Abstract:

Biomass gasification is an emerging technology for the production of synthesis gas. For realizing efficient operation of the biomass gasification process, a robust mechanism for evaluation of its energy efficiency is vital. In this context, exergy based analysis has been getting more attention from researchers over the conventional energy based analysis because of its capability to encompasses the effect of all the irreversibilities present in a process. In this study, the exergy analysis of the biomass gasifier was performed in computational fluid dynamics (CFD) environment. For the model development, the designed specifications of a lab scale downdraft biomass gasifier were used. The reaction sets were imported from species transport model. A code for exergy analysis was written in custom field function (CFF). The designed model achieved syngas composition of 1:1.55 and gasification temperature of 11000C compared to reported work in literature. In addition, the exergy analysis algorithm helped in evaluating the performance of downdraft biomass gasifier by analysing all three types of exergy, physical exergy, chemical exergy, and mixing exergy.

Keywords: Downdraft biomass gasifier, Computational fluid dynamics, Physical exergy, Chemical exergy, Mixing exergy, Custom field function